

CP and Lepton-Number Violation in GUT Neutrino Models with Abelian Flavour Symmetries

John Ellis¹, Mario E. Gómez² and Smaragda Lola³

¹ Theory Division, CERN, CH-1211 Geneva 23, Switzerland

² Departamento de Física Aplicada, University of Huelva, 21071 Huelva, Spain

³ Department of Physics, University of Patras, GR-26500 Patras, Greece

ABSTRACT

We study the possible magnitudes of CP and lepton-number-violating quantities in specific GUT models of massive neutrinos with different Abelian flavour groups, taking into account experimental constraints and requiring successful leptogenesis. We discuss SU(5) and flipped SU(5) models that are consistent with the present data on neutrino mixing and upper limits on the violations of charged-lepton flavours and explore their predictions for the CP-violating oscillation and Majorana phases. In particular, we discuss string-derived flipped SU(5) models with selection rules that modify the GUT structure and provide additional constraints on the operators, which are able to account for the magnitudes of some of the coefficients that are often set as arbitrary parameters in generic Abelian models.

1 Introduction

In recent years, several experiments have provided convincing evidence for neutrino oscillations [1, 2, 3, 4, 5], together with important information on the neutrino mass differences and mixing angles [6]. It has now been established that the atmospheric neutrino mixing angle, θ_{23} , is large, with a central value $\sim \pi/4$, so that $0.31 \leq \sin^2 \theta_{23} \leq 0.72$. The solar MSW angle θ_{12} [7] is also large, but not maximal, with $\sin^2 \theta_{12} \sim 0.3$. Upper limits from the CHOOZ experiment, in particular, establish that the third mixing angle, θ_{13} , must be small, with a present upper limit of $\sin^2 \theta_{13} \leq 0.1$ [8]. Finally, experiments have established the following ranges for the mass differences: $\Delta m_{atm}^2 \sim 2.5 \cdot 10^{-3} eV^2$ and $\Delta m_{sol}^2 \sim 8 \cdot 10^{-5} eV^2$ [6].

These important results leave several questions open for model builders to consider:

- Is the atmospheric neutrino mixing indeed maximal?
- How large is the solar neutrino mixing, and can it be related to mixing among quarks?
- What is the pattern of masses for the neutrinos?
- What is the magnitude of θ_{13} ?
- Is there significant CP violation in the neutrino and charged-lepton sectors?

In this paper we study, in particular, the answers to the last two questions that are provided by models that propose different answers to the first three questions.

The existence of neutrino masses and oscillations may have further consequences. For example, the decays of heavy neutrinos may lead to leptogenesis, which would impose additional constraints on CP-violating phases and on the magnitudes of certain neutrino Yukawa couplings [9]. These should be large enough to generate a sufficient net lepton number, but not above the value that would erase any generated asymmetry through equilibration effects. Also, mixing in the charged-lepton sector is enhanced by radiative corrections in supersymmetric models that mix the sleptons, contributing via loop diagrams to rare decays and flavour conversions [10, 11]. The rates for such processes mediated by sparticles may be large and close to the current experimental bounds in many supersymmetric models. Moreover, the possibility of CP-violation is crucial in this analysis [12] and additional CP-violating quantities may be observable in the charged-lepton sector. The model parameters that would be responsible for leptogenesis, flavour and CP violation in charged-lepton processes are different from those measurable in neutrino oscillation experiments, and also motivate this paper.

As we discuss below, the predictions for these additional parameters vary in different models. However, there are also several correlations. A combined analysis, using all available processes, could give significant constraints on models, and even exclude certain classes of models. The joint study of phases, CP and lepton-flavour violation is a central issue in this programme, and its better understanding is the central goal of this work.

The fact that the fermion mass matrices exhibit a hierarchical structure suggests that they are generated by an underlying flavour symmetry for which the simplest possibility would be an Abelian family symmetry. In such a case, one can parametrize the charges of the Standard Model fields under the symmetry as in Table 1. The Higgs charges are chosen so that the terms $f_3 f_3^c H$ (where f stands for a generic fermion, the subscript 3 denotes the third family, and H denotes either H_1 or H_2) have zero net charge whereas other terms have non-zero charges. Then, in general only the (3,3) element of the associated mass matrix will be non-zero as long as the U(1) symmetry remains unbroken. The remaining matrix elements may be generated

when the U(1) symmetry is spontaneously broken [13, 14] by fields θ , $\bar{\theta}$ that are singlets of the Standard Model gauge group, with U(1) charges that are in most cases taken to be ± 1 , respectively. Here we assume them to have equal vacuum expectation values (vev's). The suppression factor for each entry depends on the family charge: the higher the net U(1) charge of a term $f_i f_j^c H$, the higher the power n in the non-renormalisable term $f_i f_j^c H \left[\left(\frac{\langle \theta \rangle}{M} \right)^n \text{ or } \left(\frac{\langle \bar{\theta} \rangle}{M} \right)^n \right]$ that has zero charge, where M is a high mass scale that is assumed to be much larger than $\langle \theta \rangle = \langle \bar{\theta} \rangle$. The $f_3 f_3^c H$ couplings are not suppressed, because they have no net charge.

	Q_i	u_i^c	d_i^c	L_i	e_i^c	ν_i^c	H_2	H_1
U(1)	α_i	β_i	γ_i	c_i	d_i	e_i	$-\alpha_3 - \beta_3$	$-\alpha_3 - \gamma_3$

Table 1: Notation for possible U(1) charges of the various Standard Model fields, where i is a generation index.

Whilst such a family symmetry provides a promising origin for a hierarchical pattern of fermion masses, in order to go further it is necessary to specify the charges of the quarks, charged leptons and neutrinos [15]. In principle, one can fit the observed masses and mixing angles by choices of flavour charges that are not constrained by additional symmetries. However, the structure of the Standard Model is suggestive of an underlying unification relating quark and lepton multiplets, as occurs in various GUT models. In such a case, it is important to try to understand the different mass and mixing patterns and other correlations predicted by different GUTs, and the resulting patterns of CP and lepton-flavour violation in particular. This is the primary focus of this paper. Since particles in the same multiplet of a GUT group have the same charge, the predictions and correlations between observables will in general be different for different GUTs and charge assignments.

A crucial question when studying flavour symmetries is whether these are indeed *Abelian*, as described above, or *non-Abelian*. In the case of an Abelian flavour symmetry, taking predictions for the masses and mixings *only* from the flavour and GUT structure and assuming that unknown numerical coefficients are generically $\mathcal{O}(1)$ leads in the simplest and apparently more natural neutrino models to large mass hierarchies and unacceptably small solar mixing, which is correlated with the hierarchies of charged-lepton masses [16]. Large solar mixing, as required by the experimental data, has therefore to arise either from the right-handed neutrino sector (as may arise, for instance, in see-saw models with dominance by a single right-handed singlet neutrino, and other zero-determinant solutions), or by imposing more U(1) symmetries and/or introducing more fields. However, this strategy introduces additional model dependence and loses predictivity. On the other hand, large atmospheric mixing is naturally predicted in a wide class of Abelian models, and non-Abelian flavour symmetries typically predict naturally large angles for both solar and atmospheric neutrinos [17, 18].

Since there is no charge quantisation in Abelian groups, contrary to the non-Abelian case, the symmetry cannot determine alone the numerical values of the mass-matrix elements and hence the mixing angles and phases. Nevertheless, information on the phases and values of the coefficients can be inferred phenomenologically, and individual Abelian models may be used to make interesting qualitative predictions, just as they have for the mixing angles, based on the powers of the small parameters $\langle \theta \rangle / M$, $\langle \bar{\theta} \rangle / M$ that are allowed by the symmetries. However, any predictivity requires the existence of stable solutions where a small change in the parameters does not change drastically the predictions. Non-Abelian symmetries are more predictive in

this respect. However, once the symmetry is broken (as is required to generate large lepton mass hierarchies) this predictivity is to a certain extent lost. Even in this case, therefore, the phases are derived by a combination of theoretical and phenomenological considerations, again in a model-dependent way.

The fact that neutrinos have masses and mix with each other like quarks also implies that, in principle, we can expect non-negligible CP-violation in the neutrino sector. This may manifest itself in several different ways in low-energy neutrino physics, including the Maki-Nakagawa-Sakata (MNS) oscillation phase δ and two possible Majorana phases. Additional phases arise in extensions of the light-neutrino sector to include either heavy singlet neutrinos and/or charged leptons. For example, even the minimal three-generation see-saw model has 6 independent CP-violating phases, and leptogenesis is independent of the light-neutrino phases, in particular. On the other hand, some of the phases on which leptogenesis does depend may in principle be observable in the charged-lepton sector, in the presence of low-energy supersymmetry. As we discuss below, these observables may take very different values in classes of models that fit the present neutrino data equally well.

The structure of this paper is as follows. In Section 2 we discuss the neutrino and charged-lepton observables for which we investigate the predictions of various GUTs with Abelian flavour symmetries. The specific GUT models and their predictions are discussed in Section 3. Our conclusions are set out in Section 4, and appendices present details of the specific GUTs studied.

2 Observables in the Lepton Sector

2.1 Neutrino Observables

The mixing matrices $V_{e,D}, U_{R,\nu}$ that yield physical CP and flavour violating observables are those making the following diagonalisations:

$$V_e^T Y_e Y_e^\dagger V_e^* = \text{Diag}(y_e^2, y_\mu^2, y_\tau^2), \quad (1)$$

$$V_D^T Y_\nu Y_\nu^\dagger V_D^* = \text{Diag}(y_\nu^2, y_\nu^2, y_\nu^2), \quad (2)$$

$$U_R^T M_{RR} U_R = \text{Diag}(M_1, M_2, M_3), \quad (3)$$

$$U_\nu^T m_{eff} U_\nu = \text{Diag}(m_{\nu_1}, m_{\nu_2}, m_{\nu_3}), \quad (4)$$

where $Y_{e,\nu}$ stand for the Yukawa couplings of neutrinos and charged leptons respectively, and M_{RR} is the heavy Majorana neutrino mass matrix, which we assume to be three-dimensional (for a review see [19]). The effective neutrino mass matrix is:

$$m_{eff} \approx m_D^\nu \frac{1}{M_{RR}} m_D^{\nu T}. \quad (5)$$

In terms of the above matrices, the Maki-Nakagawa-Sakata (MNS) matrix becomes

$$U_{MNS} \equiv U = V_e U_\nu^\dagger, \quad (6)$$

and can be parametrized as:

$$U = \text{diag}(e^{i\delta_e}, e^{i\delta_\mu}, e^{i\delta_\tau}) \cdot V \cdot \text{diag}(e^{-i\phi_1/2}, e^{-i\phi_2/2}, 1), \quad (7)$$

where

$$V = \begin{pmatrix} c_{12}c_{13} & s_{12}c_{13} & s_{13}e^{-i\delta} \\ -c_{23}s_{12} - s_{23}s_{13}c_{12}e^{i\delta} & c_{23}c_{12} - s_{23}s_{13}s_{12}e^{i\delta} & s_{23}c_{13} \\ s_{23}s_{12} - c_{23}s_{13}c_{12}e^{i\delta} & -s_{23}c_{12} - c_{23}s_{13}s_{12}e^{i\delta} & c_{23}c_{13} \end{pmatrix}, \quad (8)$$

and c_{ij} and s_{ij} stand for $\cos \theta_{ij}$ and $\sin \theta_{ij}$, respectively. In this formalism, the three neutrino mixing angles and the six CP-violating phases are given by

$$\begin{aligned} \theta_{13} &= \arcsin(|U_{13}|), \quad \theta_{12} = \arctan\left(\frac{|U_{12}|}{|U_{11}|}\right), \quad \theta_{23} = \arctan\left(\frac{|U_{23}|}{|U_{33}|}\right), \\ \delta_\mu &= \arg(U_{23}), \quad \delta_\tau = \arg(U_{33}), \quad \delta = -\arg\left(\frac{U_{ii}^*U_{ij}U_{ji}U_{jj}^*}{c_{12}c_{13}^2c_{23}s_{13}} + c_{12}c_{23}s_{13}\right), \\ \delta_e &= \arg(e^{i\delta}U_{13}), \quad \phi_1 = 2\arg(e^{i\delta_e}U_{11}^*), \quad \phi_2 = 2\arg(e^{i\delta_e}U_{12}^*). \end{aligned}$$

where $i, j = 1, 2, 3$ and $i \neq j$. A useful measure of the amount of CP-violation in the oscillations of light neutrinos is the Jarlskog invariant

$$\begin{aligned} J_{CP} &= \frac{1}{2} |\text{Im}(U_{11}^*U_{12}U_{21}U_{22}^*)| = \frac{1}{2} |\text{Im}(U_{11}^*U_{13}U_{31}U_{33}^*)| \\ &= \frac{1}{2} |\text{Im}(U_{22}^*U_{23}U_{32}U_{33}^*)| = \frac{1}{2} |c_{12}c_{13}^2c_{23} \sin \delta s_{12}s_{13}s_{23}|. \end{aligned} \quad (9)$$

It is clear that different models that reproduce the experimental values of $\theta_{12,23}$ and the differences in light neutrino masses-squared may well predict different amounts of CP-violation in neutrino oscillations (9) and elsewhere. So far, experiment has provided only an upper bound on the possible magnitude of θ_{13} , and no information on δ . The magnitude of CP-violation in neutrino oscillations may even be zero, for example in models with texture zeroes in the (1,3) entries. As we see later, specific models may connect θ_{13} and δ , and also provide connections to other observables. We aim here at the differentiation of possible flavour models according to their predictions for observables in the neutrino sector - what are the expected magnitudes of θ_{13}, δ and $\phi_{2,3}$? - and elsewhere ¹. We now discuss some of the other observables in more detail.

2.2 Leptogenesis

The textures of neutrino Yukawa couplings may be constrained by the requirement of successful leptogenesis [21], which requires obtaining the correct magnitude of lepton-flavour violation

¹In order to calculate mixing angles and CP-violating phases in an automated way, we analyze the different models using the package REAP [20].

(LFV) in the decays of heavy, right-handed Majorana neutrinos via a difference between the branching ratios (BR) for heavy-neutrino decays into leptons and antileptons:

$$BR(N_L^c \rightarrow \bar{\Phi} + \ell) \neq BR(N_L^c \rightarrow \Phi + \bar{\ell}).$$

Since non-perturbative lepton- and baryon-number-violating interactions mediated by sphalerons are in thermal equilibrium up to the time of the electroweak phase transition, a non-zero lepton number gives rise to a non-zero baryon number, by sharing the lepton asymmetry $\Delta L \neq 0$ with a baryon asymmetry $\Delta B \neq 0$.

In order to avoid washout of the initial decay asymmetry by perturbative decay, inverse decay and scattering interactions, the model must satisfy an out-of-equilibrium condition, namely that the heavy-neutrino decay rate is smaller than the Hubble parameter H at temperatures of the order of the right handed neutrino masses. The tree-level width of the heavy neutrino N_i with mass M_i is: $\Gamma = [(\lambda^\dagger \lambda)_{ii}/8\pi]M_i$, which should be compared with the Hubble expansion rate $H \approx 1.7 g_*^{1/2} T^2/M_P$, (where $g_*^{MSSM} \approx 228.75$, $g_*^{SM} = 106.75$ and M_P is the Planck mass), leading to the requirement

$$\frac{(\lambda^\dagger \lambda)_{ii}}{14\pi g_*^{1/2}} M_P < M_i.$$

Here, $\lambda \equiv Y'_\nu$ denotes the neutrino Yukawa matrix in the basis where the Majorana masses M_i are diagonal. This condition may be implemented more accurately by looking in detail at the Boltzmann equations, but this formula is sufficient for our purposes.

The CP-violating decay asymmetry ϵ_j in the decay of a heavy-neutrino flavour j arises from the interference between tree-level and one-loop amplitudes, and is

$$\epsilon_j = \frac{1}{(8\pi Y'_\nu{}^\dagger Y'_\nu)_{jj}} \sum_{i \neq j} \text{Im} [((Y'_\nu{}^\dagger Y'_\nu)_{ji})^2] f\left(\frac{M_j^2}{M_i^2}\right), \quad (10)$$

where the kinematic function

$$f(y) = \sqrt{y} \left[\frac{1}{1-y} + 1 - (1+y) \ln\left(\frac{1+y}{y}\right) \right].$$

The first term in $f(y)$ arises from self-energy corrections, while the second and third terms arise from the one-loop vertex. For models with degenerate Majorana masses, one expects a resonant enhancement of the lepton asymmetry, since in this case $y \sim 1$ and

$$f(y) \sim -\frac{|M_i|}{2(|M_j| - |M_i|)}. \quad (11)$$

This will be manifest in some of the examples below.

The lepton asymmetry produced by the decays of the heavy neutrinos is in general diluted partially by lepton-number-violating processes [21]. The washout factor κ_i is approximately

$$\kappa_i(\tilde{m}_i) \simeq 0.3 \left(\frac{10^{-3}\text{eV}}{\tilde{m}_i} \right) \left(\log \frac{\tilde{m}_i}{10^{-3}\text{eV}} \right)^{-0.6}, \quad (12)$$

where

$$\tilde{m}_i = (M'_{RR}{}^\dagger M'_{RR})_{ii}/|M_i|, \quad (13)$$

and the primes denote the basis where the right-handed neutrino mass matrix is diagonal.

Then, for a supersymmetric model, the lepton and baryon asymmetries are given by

$$\left(\frac{n_L}{s}\right) \simeq 0.8 \times 10^{-2} \kappa_i \epsilon_i \frac{1}{\Delta}, \quad (14)$$

$$\left(\frac{n_B}{s}\right) \simeq -2.8 \times 10^{-3} \kappa_i \epsilon_i \frac{1}{\Delta}, \quad (15)$$

$$\eta_B \simeq -0.02 \kappa_i \epsilon_i \frac{1}{\Delta}, \quad (16)$$

where the entropy of the co-moving volume s is given by $s = (2/45)g_*\pi^2 T^3$, and $g_* = 228.75$ refers to the effective number of relativistic degrees of freedom contributing to the entropy in our supersymmetric model.

In the above relations, Δ is a dilution factor that appears due to entropy production from symmetry breaking and an inflationary phase. This effect has been studied in [22], in the context of the breaking of $SU(5) \times U(1)$ when a singlet field Φ gets a vev. In this case, the dilution factor is [23] $\Delta = \frac{s(R_{d\Phi})}{s(R_{d\eta})} \left(\frac{R_{d\Phi}}{R_{d\eta}}\right)^3 \sim \frac{V^3 m_\eta^{3/2}}{\alpha_\Phi^{1/2} m_{SUSY}^3 M_P^3}$. Here, the Φ decay rate is given by

$\Gamma_\Phi = \alpha_\Phi \frac{m_{SUSY}^3}{V^2}$, V is the scale where the vev of the Higgs $\mathbf{10}$ and $\overline{\mathbf{10}}$ break the flipped-SU(5) group, m_η is the inflaton mass, and m_{SUSY} is the supersymmetry breaking scale.

Successful leptogenesis would require [25]:

$$\eta_B = (6.15 \pm 0.25) \times 10^{-10}. \quad (17)$$

Clearly, $\kappa_i/\Delta < 1$ in general and a model with too small a value of ϵ_i would not be valid. However, as we discuss below, this is not the case in the models we study, which generally require $\Delta \gg 1$ in order to provide a successful scheme of leptogenesis. An alternative to invoking a large dilution factor would be to adopt a wider range of neutrino Yukawa couplings and Majorana masses that can lead to consistent solutions.

The impact of flavour effects in leptogenesis has also been considered in [26] and more recently in [27], and may affect the results by factors of ~ 2 . Since the conclusions of our paper are not affected by the possible presence of such factors, we will not proceed with more detailed considerations in this direction.

2.3 Charged-Lepton-Flavour Violation

In the context of low-energy supersymmetry, mixing in the neutrino sector also generates mixing in the sleptons via loop corrections, contributing to rare decays and lepton-flavour conversions. We evaluate these effects in the context of the CMSSM, where the soft supersymmetry-breaking masses of the charged and neutral sleptons are assumed to be universal at the GUT scale, and may be written in diagonal form with a common value m_0 . Off-diagonal entries in the slepton mass matrix m_L^2 are then generated radiatively by the renormalization-group evolution from the GUT scale M_{GUT} .

The branching ratios for LFV decays can be described well by a single-mass-insertion approximation [28, 29]:

$$BR(l_i \rightarrow l_j \gamma) \approx \frac{\alpha^3}{G_F^2} \mathcal{F}(m_0, M_{1/2}, \mu) |m_{\tilde{L}_{ij}}^2|^2 \tan^2 \beta, \quad (18)$$

where \mathcal{F} is a function of the soft supersymmetry-breaking masses fixed at the high scale M_{GUT} , and $i \neq j$ are generation indices. In the commonly-used approximation for solving the renormalisation-group equations of a single intermediate right-handed neutrino threshold, the mass corrections are related to the neutrino Yukawa couplings by [30]

$$m_{\tilde{L}_{ij}}^2 = \kappa \sum_k \bar{Y}_\nu^{ik} (\Delta t + \Delta \ell_k) (\bar{Y}_\nu^{jk})^*, \quad (19)$$

where \bar{Y}_ν is the Dirac neutrino Yukawa matrix in a basis where both the heavy-Majorana and charged-lepton couplings become diagonal, and

$$\kappa = -6m_0^2 - 2A_0^2, \quad \Delta t = \ln(M_{GUT}/M_3)/16\pi^2, \quad \Delta \ell_k = \ln(M_3/M_k)/16\pi^2. \quad (20)$$

where M_i with $i = 1, 2, 3$ denote the Majorana neutrino masses assuming $M_1 < M_2 < M_3$.

This result is not very accurate, but it is a useful approximation for obtaining analytical expressions for lepton-flavour-violating decay rates [31]. In the analysis that follows we assume for simplicity that $A_0 = 0$. If $A_0 \neq 0$, this parameter would also be similarly renormalized, via

$$(\delta A_e)_{ij} \approx -\frac{1}{8\pi^2} A_0 Y_{e_i} (\bar{Y}_\nu \bar{Y}_\nu^\dagger)_{ij} \log \frac{M_{GUT}}{M_i}. \quad (21)$$

The extra suppression due to Y_e and the form of κ indicate that, unless A_0 becomes much larger than m_0 , our conclusions will be qualitatively unchanged.

Another lepton-number-violating observable is $\mu \rightarrow e$ conversion on a nucleus, which has a rate

$$\begin{aligned} R(\mu^+ T i \rightarrow e^+ T i) &\approx \frac{\alpha}{3\pi} \frac{E_e p_e}{m_\mu^2} \frac{Z F_c^2}{C f(A, Z)} BR(\mu \rightarrow e \gamma) \\ &\approx 5.6 \times 10^{-3} BR(\mu \rightarrow e \gamma). \end{aligned} \quad (22)$$

This process is very interesting, despite the relative suppression by about two orders of magnitude, because of the accuracy possible in future measurements of this process. Within the framework discussed here, a similar suppression is expected for the decay $\mu \rightarrow 3e$,

$$\frac{\Gamma(\mu^+ \rightarrow e^+ e^+ e^-)}{\Gamma(\mu^+ \rightarrow e^+ \gamma)} \approx 6 \times 10^{-3}. \quad (23)$$

However, the present experimental bound on this branching ratio is relatively weak, and the prospects for significant improvement are more distant. It should be noted, though, that this decay does offer the possibility of observing a T-violating asymmetry, which might be observable if $\mu \rightarrow e \gamma$ occurs with a rate close to the present experimental upper limit. The flavour-violating decays $\tau \rightarrow e \gamma$ and $\mu \gamma$ are also potentially interesting. They are governed by formulae similar to those above, and later we present some results for them.

3 GUTs with Abelian Flavour Symmetries

As mentioned in the Introduction, we focus in this work on Abelian flavour symmetries, since they are simple and arise naturally in a wide class of models. Moreover, understanding Abelian symmetries is a first step towards the understanding of non-Abelian symmetries. Indeed, by combining two or more Abelian symmetries and introducing more than one field whose vev determines the expansion parameter of the mass matrices, one can simulate to some extent the picture that one would obtain from a non-Abelian structure.

3.1 SU(5)

The first GUT group we analyze is SU(5), whose minimal matter field content is three families of $(Q, u^c, e^c)_i \in 10$ representations of SU(5), three families of $(L, d^c)_i \in \bar{5}$ representations, and heavy right-handed neutrinos $N_L^c \equiv \nu_R$ in singlet representations. Only two heavy $N_L^c \equiv \nu_R$ fields are needed to provide two non-zero masses for light neutrinos, as required by experiment, and more than three are present in some models. However, in what follows, we assume that there are also just three heavy $N_L^c \equiv \nu_R$ fields. This model has the following properties that are important for our analysis:

- (i) the up-quark mass matrix is symmetric,
- (ii) the charged-lepton mass matrix is the transpose of the down-quark mass matrix, which relates the mixing of the left-handed leptons to that of the right-handed down-type quarks. Since the CKM mixing in the quark sector is due to a mismatch between the mixing of the left-handed up- and down-type quarks, it is independent of mixing in the lepton sector. In particular, in SU(5) the large mixing angle that is observed in atmospheric neutrino oscillations can easily be consistent with the observed small V_{CKM} mixing. Most importantly,
- (iii) it is clear from the SU(5) representation structure that the Abelian flavour charges of the fermions $(Q, u^c, e^c)_i$ in the same 10 representation must be identical, as must the charges of the $(L, d^c)_i$ in the same $\bar{5}$ representation. This is the type of correlation that we seek to test by examining model predictions for flavour and CP violation in the generalised lepton sector.

There are several possibilities for the Abelian flavour charges, that are motivated by theoretical considerations such as anomaly cancellation [32] as well as phenomenological arguments. Within this framework, one may address questions such as:

- How close to maximal is the atmospheric mixing?
- How large is the solar mixing?
- How large are θ_{13} and δ ?
- At which level is mixing controlled by the hierarchies of charged-lepton masses, and how strong is the influence from the heavy right-handed neutrino sector?
- What statements can be made about other observables?

There are several viable sets of textures that we analyze for answers to these questions. Taking into account the above-mentioned constraints arising from the SU(5) multiplet structure (symmetric up-quark mass matrix, and M_ℓ the transpose of M_{down}), the mass matrices are

constrained to the forms

$$\mathcal{M}_u \propto \begin{pmatrix} \epsilon^{|2x|} & \epsilon^{|x+b|} & \epsilon^{|x|} \\ \epsilon^{|x+b|} & \epsilon^{|2b|} & \epsilon^{|b|} \\ \epsilon^{|x|} & \epsilon^{|b|} & 1 \end{pmatrix}, \quad M_{down} \propto \begin{pmatrix} \bar{\epsilon}^{|x+y|} & \bar{\epsilon}^{|x+a|} & \bar{\epsilon}^{|x|} \\ \bar{\epsilon}^{|y+b|} & \bar{\epsilon}^{|a+b|} & \bar{\epsilon}^{|b|} \\ \bar{\epsilon}^{|y|} & \bar{\epsilon}^{|a|} & 1 \end{pmatrix}, \quad M_\ell \propto \begin{pmatrix} \bar{\epsilon}^{|x+y|} & \bar{\epsilon}^{|y+b|} & \bar{\epsilon}^{|y|} \\ \bar{\epsilon}^{|x+a|} & \bar{\epsilon}^{|a+b|} & \bar{\epsilon}^{|a|} \\ \bar{\epsilon}^{|x|} & \bar{\epsilon}^{|b|} & 1 \end{pmatrix}, \quad (24)$$

where $a = Q_2^{\bar{5}} - Q_3^{\bar{5}}$, $b = Q_2^{10} - Q_3^{10}$, $x = Q_1^{10} - Q_3^{10}$, $y = Q_1^{\bar{5}} - Q_3^{\bar{5}}$. We note that, by assumption, the (3, 3) entries in all the mass matrices are $\mathcal{O}(1)$, as would be suitable for large $\tan\beta$ ², and we have assumed that the flavour charges of the two supersymmetric Higgs fields are the same. Since we know that the (3,3) entry in the charged-lepton mass matrix is the largest one, we have simplified our considerations by taking a zero Higgs flavour charge³.

3.2 An example with large $\tan\beta$

An interesting possibility is that *maximal atmospheric mixing arises from the charged-lepton sector*. In this case, the (2,3) and (3,3) lepton entries are comparable, and $a = 0$. The resulting mass matrices have been discussed in the literature, e.g., in [16]. The choice $|b| = 2$ leads to the correct m_s/m_b ratio, while requiring correct (1,2) quark mixing fixes $|x| = 3$ in the down mass matrix⁴ and $|y|$ is fixed by the down and charged-lepton mass hierarchies. Thus, one obtains finally mass matrices of the form [16, 33]:

$$\mathcal{M}_u \propto \begin{pmatrix} \bar{\epsilon}^6 & \bar{\epsilon}^5 & \bar{\epsilon}^3 \\ \bar{\epsilon}^5 & \bar{\epsilon}^4 & \bar{\epsilon}^2 \\ \bar{\epsilon}^3 & \bar{\epsilon}^2 & 1 \end{pmatrix}, \quad M_{down} \propto \begin{pmatrix} \bar{\epsilon}^4 & \bar{\epsilon}^3 & \bar{\epsilon}^3 \\ \bar{\epsilon}^3 & \bar{\epsilon}^2 & \bar{\epsilon}^2 \\ \bar{\epsilon} & 1 & 1 \end{pmatrix}, \quad M_\ell \propto \begin{pmatrix} \bar{\epsilon}^4 & \bar{\epsilon}^3 & \bar{\epsilon} \\ \bar{\epsilon}^3 & \bar{\epsilon}^2 & 1 \\ \bar{\epsilon}^3 & \bar{\epsilon}^2 & 1 \end{pmatrix}, \quad (25)$$

where a single expansion parameter has been used to reproduce the fermion mass hierarchies⁵.

As is clear from the form of the charged-lepton mass matrix, unlike what happens for the atmospheric mixing, the solar mixing cannot be obtained from the charged-lepton sector. In this case, it has to arise from the neutrino sector, exploiting the see-saw structure. It is interesting to observe the *a priori* large value of θ_{13} given by the charged-lepton sector - indeed, θ_{13} may even be too large - but the overall (1,3) lepton mixing can be reduced either by a numerical coefficient, or by a cancellation between the charged-lepton and neutrino mass matrices. In fact, comparing the textures for maximal and non-maximal mixing, we see that, due to the different magnitudes of the neutrino mixing angles entering in the Jarlskog invariant, one can expect in principle different inter-correlations and predictions for CP-violation, even before looking in detail at the heavy right-handed neutrino sector and its influence on m_{eff} .

In general, of course, both the mass structure and the mixings of neutrinos are more complicated, because of the heavy Majorana masses of the right-handed components. We assume that these arise from terms of the form $\nu_R \nu_R \Sigma$, where Σ is an $SU(3) \times SU(2) \times U(1)$ -invariant Higgs

²We look below also at examples with small $\tan\beta$.

³The conditions for anomaly cancellation give further insight into the possible textures, but detailed model building goes beyond the scope of this paper.

⁴We cannot obtain the (1,2) quark mixing from the up sector, as this would lead to an unacceptably large mass for the up quark.

⁵This example gives an up-quark mass that tends to be somewhat too high, but this defect can be remedied in specific models.

field with $I_W = 0$ and a non-zero flavour U(1) charge ⁶. The possible choices for the Σ charge give a discrete spectrum of forms for the Majorana mass matrix M_{ν_R} . In the case of a single Σ field and assuming a zero Higgs charge and left-handed lepton charges as above, we have:

$$m_D^\nu \propto \begin{bmatrix} \epsilon^{|y+n_1|} & \epsilon^{|y+n_2|} & \epsilon^{|y+n_3|} \\ \epsilon^{|a+n_1|} & \epsilon^{|a+n_2|} & \epsilon^{|a+n_3|} \\ \epsilon^{|n_1|} & \epsilon^{|n_2|} & \epsilon^{|n_3|} \end{bmatrix}, \quad (26)$$

$$M_{RR} \propto \begin{bmatrix} \bar{\epsilon}^{|2n_1+\sigma|} & \bar{\epsilon}^{|n_1+n_2+\sigma|} & \bar{\epsilon}^{|n_1+n_3+\sigma|} \\ \bar{\epsilon}^{|n_1+n_2+\sigma|} & \bar{\epsilon}^{|2n_2+\sigma|} & \bar{\epsilon}^{|n_2+n_3+\sigma|} \\ \bar{\epsilon}^{|n_1+n_3+\sigma|} & \bar{\epsilon}^{|n_2+n_3+\sigma|} & \bar{\epsilon}^{|2n_3+\sigma|} \end{bmatrix}, \quad (27)$$

where the charges n_i are the U(1) charges of the right-handed neutrinos, and σ is the U(1) charge of the field Σ . Unlike what happens for the charged leptons, where the (3,3) entry is the largest one, the large entry in M_{RR} can be in any position in the matrix, depending on the relative charges of Σ and the right-handed neutrinos.

We recall that the effective light-neutrino mass matrix is given by

$$m_{eff} \approx m_D^\nu \frac{1}{M_{RR}} m_D^{\nu T}.$$

Its diagonalization relative to the charged-lepton mass matrix (which is the transpose of the down-type quark mass matrix) determines the MNS mixing matrix. In the case of a zero flavour charge for the Higgs, the mass matrix is determined by the flavour charges of the left-handed neutrinos, which in SU(5) are the same as those of the right-handed down quarks. The effective light-neutrino mass matrix then has the structure

$$m_{eff} \propto \begin{pmatrix} \bar{\epsilon}^{|2y|} & \bar{\epsilon}^{|y+a|} & \bar{\epsilon}^{|y|} \\ \bar{\epsilon}^{|y+a|} & \bar{\epsilon}^{|2a|} & \bar{\epsilon}^{|a|} \\ \bar{\epsilon}^{|y|} & \bar{\epsilon}^{|a|} & 1 \end{pmatrix}. \quad (28)$$

From the values of a and y obtained from the charged-fermion mass hierarchies, we then conclude that

$$m_{eff} \propto \begin{pmatrix} \bar{\epsilon}^2 & \bar{\epsilon} & \bar{\epsilon} \\ \bar{\epsilon} & 1 & 1 \\ \bar{\epsilon} & 1 & 1 \end{pmatrix}, \quad m_D^\nu \propto \begin{pmatrix} \bar{\epsilon}^{|1\pm n_1|} & \bar{\epsilon}^{|1\pm n_2|} & \bar{\epsilon}^{|1\pm n_3|} \\ \bar{\epsilon}^{|n_1|} & \bar{\epsilon}^{|n_2|} & \bar{\epsilon}^{|n_3|} \\ \bar{\epsilon}^{|n_1|} & \bar{\epsilon}^{|n_2|} & \bar{\epsilon}^{|n_3|} \end{pmatrix}, \quad (29)$$

which can potentially lead to large solar and atmospheric neutrino mixing (the expansion parameter of the Dirac neutrino mass matrix is in principle similar to that for the up quarks, since these particles couple to the same Higgs field, but there can be deviations from this).

A working example along these lines can be obtained by the following choice of charges:

$$n_1 = 2, n_2 = -1, n_3 = 1, \sigma = -1. \quad (30)$$

Using the indicative choices of the coefficients a_{ij}^x shown in Table 2, we have calculated the relevant observables shown in Table 3. The expansions in $\bar{\epsilon}$ are obtained by using similar techniques as in Ref. [34]. Altering the coefficients a_{ij}^x would affect the numerical values appearing in Table 3, but not the powers of $\bar{\epsilon}$.

⁶Note that Σ is a singlet that enters only in the heavy Majorana mass textures. It is not the same as the θ field that generates the light fermion masses.

	Parameters in an SU(5) model with large $\tan\beta$
Charged leptons	$a_{12}^e = 0.6, a_{13}^e = 0.9, a_{22}^e = 1.2, a_{23}^e = -0.5e^{i\pi/3}, a_{31}^e = 0.7, a_{32}^e = 0.6, a_{33}^e = 0.4$
m_D^ν	$a_{12}^\nu = 1.3, a_{21}^\nu = -1.3, a_{22}^\nu = 0.7, a_{23}^\nu = 1.8e^{i\pi/5}, a_{32}^\nu = 0.7, a_{33}^\nu = 0.5$
M_{RR}	$a_{22}^N = 1, a_{33}^N = 1.8$

Table 2: Choice of coefficients that reproduce the fermion data for an SU(5) model with large $\tan\beta$. Coefficients not listed in the Table are set to unity.

Observables	Series Expansions	Numerical Values
m_{ν_3} (eV)	$0.23\bar{\epsilon} + 0.35\bar{\epsilon}^3 + 0.66\bar{\epsilon}^5$	0.05(0.047)
m_{ν_1}/m_{ν_3}	$0.85\bar{\epsilon} - 0.51\bar{\epsilon}^2 - 1.92\bar{\epsilon}^3$	0.13(0.17)
m_{ν_2}/m_{ν_3}	$0.84\bar{\epsilon} + 0.52\bar{\epsilon}^2 - 1.93\bar{\epsilon}^3$	0.17(0.17)
M_1/M_3	$1.8\bar{\epsilon} - 1.21\bar{\epsilon}^2 - 0.34\bar{\epsilon}^3$	0.31(0.36)
M_2/M_3	$1 + 1.21\bar{\epsilon}^2 + 3.62\bar{\epsilon}^3$	0.95(1)
$m_{\nu_{ee}}$ (eV)	$0.56\bar{\epsilon}^3 - 2.96\bar{\epsilon}^5 + 12.94\bar{\epsilon}^7$	0.0043(0.0044)
θ_{23}	$0.92 - 1.39\bar{\epsilon}^2 - 1.65\bar{\epsilon}^4$	0.85(0.92)
θ_{12}	$0.78 - 1.43\bar{\epsilon} + 3.62\bar{\epsilon}^3$	0.53(0.78)
θ_{13}	$0.96\bar{\epsilon} - 2.92\bar{\epsilon}^3 + 3\bar{\epsilon}^5$	0.17(0.19)
δ	$3.72 - 0.18\bar{\epsilon} + 6.1\bar{\epsilon}^2$	4.3(3.72)
J_{CP}	$0.093\bar{\epsilon} - 0.26\bar{\epsilon}^3 - 0.57\bar{\epsilon}^5$	0.017(0.019)
ϕ_1	$5.6 - 3.43\bar{\epsilon} + 19.3\bar{\epsilon}^2$	5.71(5.6)
ϕ_2	$2.46 + 2.68\bar{\epsilon} + 19.3\bar{\epsilon}^2$	3.93(2.46)
ϵ_1	$0.086\bar{\epsilon}^3 - 0.04\bar{\epsilon}^4 + 0.3\bar{\epsilon}^5$	$4.1 \times 10^{-4}(0.69 \times 10^{-4})$
ϵ_2	$-0.005\bar{\epsilon}^3 + 0.02\bar{\epsilon}^4 + \frac{0.026\bar{\epsilon} + 0.33\bar{\epsilon}^2}{2.42 + 7.24\bar{\epsilon}}$	0.007 (0.0048)
ϵ_3	$0.005\bar{\epsilon}^3 - 0.02\bar{\epsilon}^4 + \frac{0.026\bar{\epsilon} + 0.33\bar{\epsilon}^2}{2.42 + 7.24\bar{\epsilon}}$	0.0063 (0.0048)
$\eta_B \times \Delta$	—	$3.16 \times 10^{-7}(2.46 \times 10^{-7})$
$\frac{16\pi^2}{\kappa} \times m_{L12}^2$	$13.1\bar{\epsilon} - 1.42\bar{\epsilon}^2 - 60\bar{\epsilon}^3$	2.2(2.6)
$BR(\mu \rightarrow e\gamma) \times \frac{1}{(\tan\beta)^2}$	—	$5.3 \times 10^{-11}(7.4 \times 10^{-11})$
$\frac{16\pi^2}{\kappa} \times m_{L13}^2$	$11.5\bar{\epsilon} + 0.84\bar{\epsilon}^2 - 41\bar{\epsilon}^3$	2.2(2.3)
$BR(\tau \rightarrow e\gamma) \times \frac{1}{(\tan\beta)^2}$	—	$4.4 \times 10^{-11}(5.7 \times 10^{-11})$
$\frac{16\pi^2}{\kappa} \times m_{L23}^2$	$12.7\bar{\epsilon}^2 - 2.2\bar{\epsilon}^3 - 51\bar{\epsilon}^4$	0.43(0.51)
$BR(\tau \rightarrow \mu\gamma) \times \frac{1}{(\tan\beta)^2}$	—	$2 \times 10^{-12}(2.8 \times 10^{-12})$

Table 3: Values of observables predicted in the SU(5) model with large $\tan\beta$. The rate of convergence of each expansion in $\bar{\epsilon}$ can be judged from the relative magnitudes of the expansion coefficients and by comparing the exact numerical value of the observables with that obtained by keeping only the dominant term in each expansion (given in parenthesis except for ϵ_2 and ϵ_3 , where the number in parenthesis corresponds to the full fraction).

In this example, $Y_\tau(M_{\text{GUT}}) \sim 0.6$, which can be compatible with $\tan\beta$ from 40 to 50 (taking into account the potentially large, model-dependent corrections to m_b and m_τ [35]). Moreover, a mass of $m_{\nu_3} \sim 0.05$ eV is compatible with heavy Majorana masses $\sim 10^{14}$ GeV. Specifically,

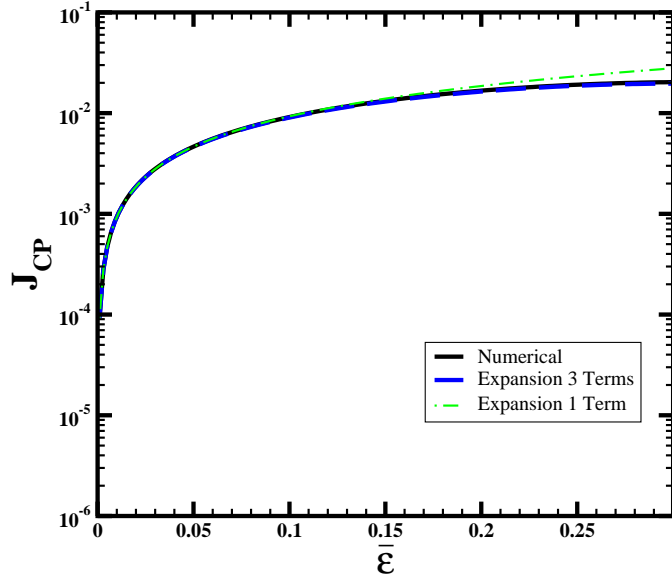


Figure 1: *The invariant J_{CP} as a function of the expansion parameter $\bar{\epsilon}$ for the case of $SU(5)$ with large $\tan\beta$. The solid line was obtained numerically while the green dot-dashed (blue dashed) line uses only the first term (three first terms) in the power expansion in $\bar{\epsilon}$.*

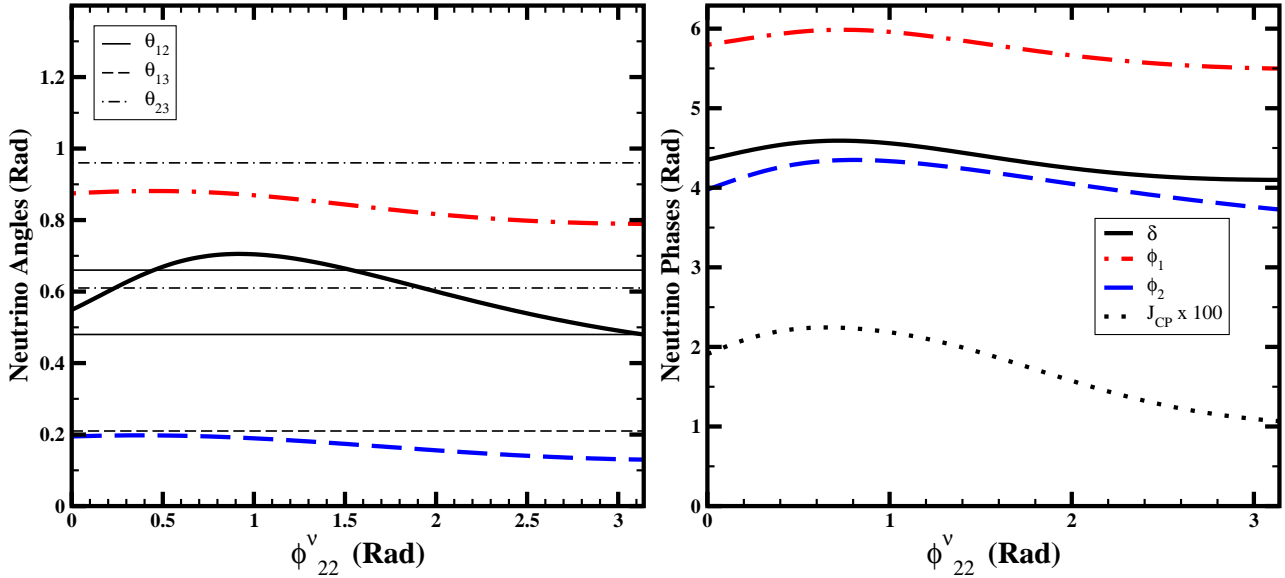


Figure 2: *The neutrino mixing angles (left) and the phases and values of the CP-violating Jarlskog invariant J_{CP} (right), as functions of the phase $\phi_{22}^\nu \equiv \text{Arg}(a_{22}^\nu)$. The experimental limits on the three neutrino angles are denoted by horizontal lines. The values of the table match the values of the figure at $\text{Arg}(a_{22}^\nu) = 0$.*

for $m_{\nu_3} = 0.05$ eV, the coefficients in Table 2 would predict $M_3 = 2.62 \times 10^{14}$ GeV. We note the following points of interest.

(i) For almost all entries there is good agreement between the precise numerical values and the dominant term in the expansions. (In the Tables, for presentation purposes, we replace $\log \bar{\epsilon}$ with its numerical value at $\bar{\epsilon} = 0.2$ in the entries for leptogenesis and charged-lepton-flavour violation, which is a good approximation for the values of ϵ of physical relevance). As seen in Fig. 1 (where we compare the numerical values of J_{CP} with those obtained by keeping the first and the three first terms in the expansions) the series expansion for J_{CP} is very accurate in the relevant range of $\bar{\epsilon}$.

(ii) The model prediction for θ_{13} is numerically smaller than θ_{12} , but not parametrically smaller. Correspondingly, as seen in Fig. 2 (left), the model prediction for θ_{13} lies not far below the present experimental upper limit. We also see in this plot that the model predictions for θ_{23} and θ_{12} lie generally near or within the bands allowed by experiment, whatever the value of the model phase parameter ϕ'_{22} .

(iii) The model prediction for δ is parametrically large and $\mathcal{O}(1)$, as seen in Fig. 2 (right). We also see that the light-neutrino Majorana phases $\phi_{1,2}$ are also generically large, and do not vary strongly with ϕ'_{22} .

(iv) Observable CP-violation is expected in neutrino oscillations, since the Jarlskog invariant scales as $\bar{\epsilon}$. Numerically, it is typically $\mathcal{O}(10^{-2})$, as also seen in Fig. 2 (right).

(v) As seen in Table 3, leptogenesis is naturally embedded in the model, and is resonantly enhanced via self-energy corrections, due to the quasi-degeneracy of the heavy Majorana neutrinos: $M_2 \sim M_3$. In this example, the self-energy contributions are almost an order of magnitude larger than the vertex corrections. The resonant behaviour is also manifest in the expansions, which are divergent when keeping only the dominant terms (due to a term of the form $\frac{1}{1+b\epsilon}$, which diverges for $\epsilon \rightarrow -1/b$). To demonstrate this, the expansions are displayed by writing separately the convergent (vertex) and the divergent (self-energy) contributions. As discussed above, in order to achieve successful leptogenesis, η_b must be in the range of eq.(17). For the values presented in Table 3, this implies a dilution factor of $\Delta \sim 500$. Alternatively, by scaling m_D^ν with global factor f_s , we could allow for different values of the dilution factor Δ . In this case, the prediction $m_{\nu_3} \sim 0.05$ eV could be preserved by also rescaling M_{RR} by a factor of f_s^2 . Then, eq. (10) indicates that ϵ would be modified by a factor f_s^2 . For the set of textures discussed in this section, by setting $f_s = 0.0441$ one could obtain η_B in the range of eq. (17) with $\Delta \sim 1$ and $M_3 \sim 5 \times 10^{11}$ GeV. In this case, the predictions for lepton flavor violation would be modified by a factor of approximately f_s^2 . For instance, the previous value of f_s would imply a prediction of $\text{BR}(\mu \rightarrow e\gamma) \sim 10^{-15} \tan\beta^2$ which is still of the experimental interest for the large values of $\tan\beta$ assumed in this model, while the predictions for $\text{BR}(\tau \rightarrow \mu\gamma)$ and $\text{BR}(\tau \rightarrow e\gamma)$ would become very small.

(vi) As also seen in Table 3, the model predicts a large rate for $\text{BR}(\mu \rightarrow e\gamma)$, close to the present experimental upper limit, as could have been expected for $\tan\beta \geq 40$. This and the other rates for lepton-flavour violation have been estimated using (18). The values of the soft terms are such that the function $\mathcal{F}(m_0, M_{1/2}, \mu)$ displays a small variation with m_0 , as seen in Fig. 1 of [31] for $A_0 = 0$, $M_{1/2} = 600$ GeV, $m_0 = 300$ GeV. In this case, $\mathcal{F} \sim 10^{-18} G_F^2 / \alpha^3$. This function could increase by two orders of magnitude if $M_{1/2}$ were decreased, but this range of values is excluded by cosmology. Alternatively, the rate could be decreased by either increasing $M_{1/2}$ and m_0 , or by reducing the Dirac neutrino Yukawa couplings, with a corresponding adjustment of the heavy Majorana masses.

(vii) More unexpected is the suppression of $BR(\tau \rightarrow \mu\gamma)$, and especially of $BR(\tau \rightarrow e\gamma)$. These suppressions arise from the form of the charged-lepton mixing matrix V_e which, in combination with the degeneracy of the heavy neutrinos, tends to align the rotated Yukawa matrix Y^ν in the base in which charged leptons are diagonal: $\bar{Y}^\nu = V_e^T Y^\nu U_N$. We return to this issue in subsequent examples.

3.3 Examples with Small $\tan\beta$

In [32], the U(1) charges were chosen so as to cancel anomalies, and several solutions were found in the small- $\tan\beta$ regime of supersymmetric theories. Restricting their attention to solutions with $c_2 = c_3$ and textures where the heavy-Majorana mass matrix can be considered as diagonal, the authors of [32] found five different fits to SU(5) models, whose detailed formulae are given in Appendix I. The choices of U(1) charges correspond to different solutions of the anomaly-cancellation conditions, and the behaviours of the fits in [32] are very dependent on this. We distinguish:

(a) *Fits 1-3*: In these fits, single right-handed neutrino dominance (SRHND) has been imposed on M_{RR} . This is achieved by choosing the charge n_1 to be a negative number between $-\sigma/2$ and 0. Using the GUT values found in Table 11 of [32], we obtain the best fits when n_1 is close to zero, as seen in Table 4.

(b) *Fits 4,5*: In these cases, we do not find fits with clear-cut SRHND. As one can see in Table 4, the required value for n_1 is still zero ⁷.

We have calculated the relevant observables, including the expected CP and charged-lepton-flavour violation, for representatives of these two classes of fits, in order to compare their behaviours for different sets of parameters within the same GUT framework. Since Fits 1-3 and 4-5 have common characteristics, we focus on one solution from each group, and work specifically with Fits 2 and 4 of [32]. The values of ϵ, σ and n_1 used in these fits are given in Table 4, and the chosen values of the numerical coefficients a_{ij} are tabulated in Tables 5 and 6 for Fits 2 and 4 of [32], respectively. The corresponding predictions for neutrino masses and mixing angles, CP and lepton-flavour violation are given in Tables 7 and 8, respectively.

The values of $\tan\beta$ for Fits 2 and 4 are obtained by using the Yukawa couplings Y_e and the experimental value of m_τ ; these lead to $\tan\beta = 2.04$ for Fit 2 and $\tan\beta = 5.15$ for Fit 4. The textures Y_ν and M_{RR} are scaled so that $m_{\nu_3} = 0.05$ eV when the largest right-handed neutrino mass becomes $M_3 = 5 \cdot 10^{14}$ GeV. For Fit 2, this implies that

$$Y_\nu \rightarrow Y_\nu \cdot 0.46 \cdot \epsilon^{-9/2}, \quad M_{RR} \rightarrow M_{RR} / \langle \Sigma \rangle \cdot 2.1 \cdot 10^{14} \cdot \epsilon^{-19/2}, \quad (31)$$

while for Fit 4

$$Y_\nu \rightarrow Y_\nu \cdot 0.42, \quad M_{RR} \rightarrow M_{RR} / \langle \Sigma \rangle \cdot 2.34 \cdot 10^{14}. \quad (32)$$

The expansions of the observables in powers of ϵ are obtained as discussed above.

⁷In principle, one could also investigate what happens for other forms of M_{RR} , since in general there might be dominant off-diagonal terms (depending on the singlet charges). However, such a study would go beyond the scope of this paper.

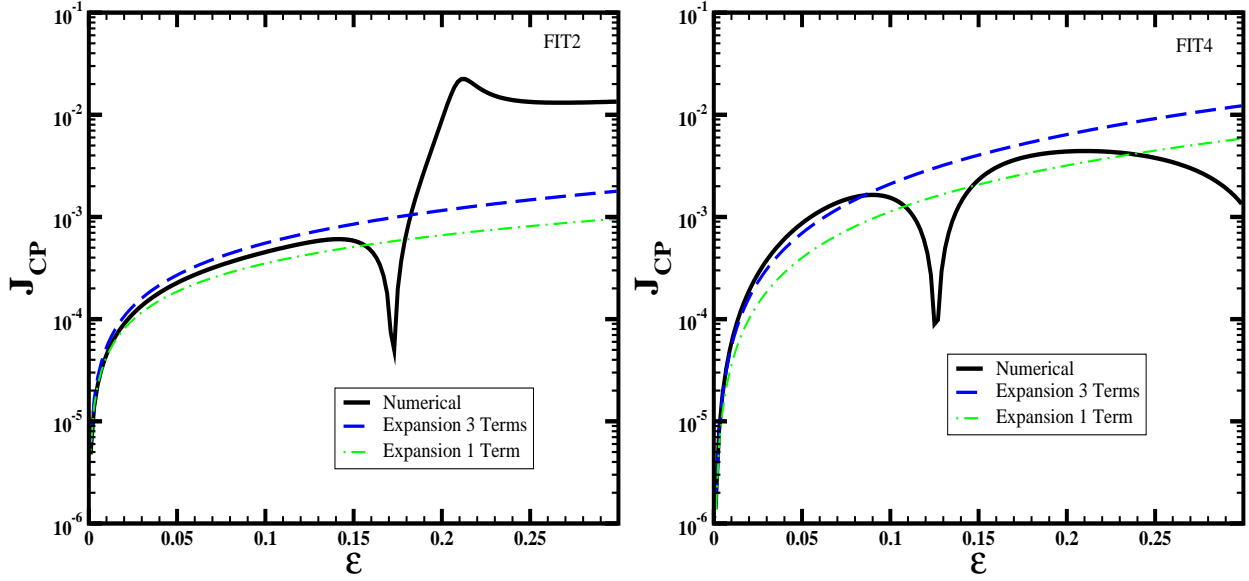


Figure 3: The Jarlskog invariant J_{CP} as a function of the expansion parameter ϵ for two $SU(5)$ models at low $\tan\beta$. The textures correspond to Fits 2 and 4 of [32] for the values of the coefficients a_{ij} in Tables 5 and 6. The solid line was obtained numerically while the dot-dash (dash) line uses only the first term (three first terms) in the power expansion in ϵ .

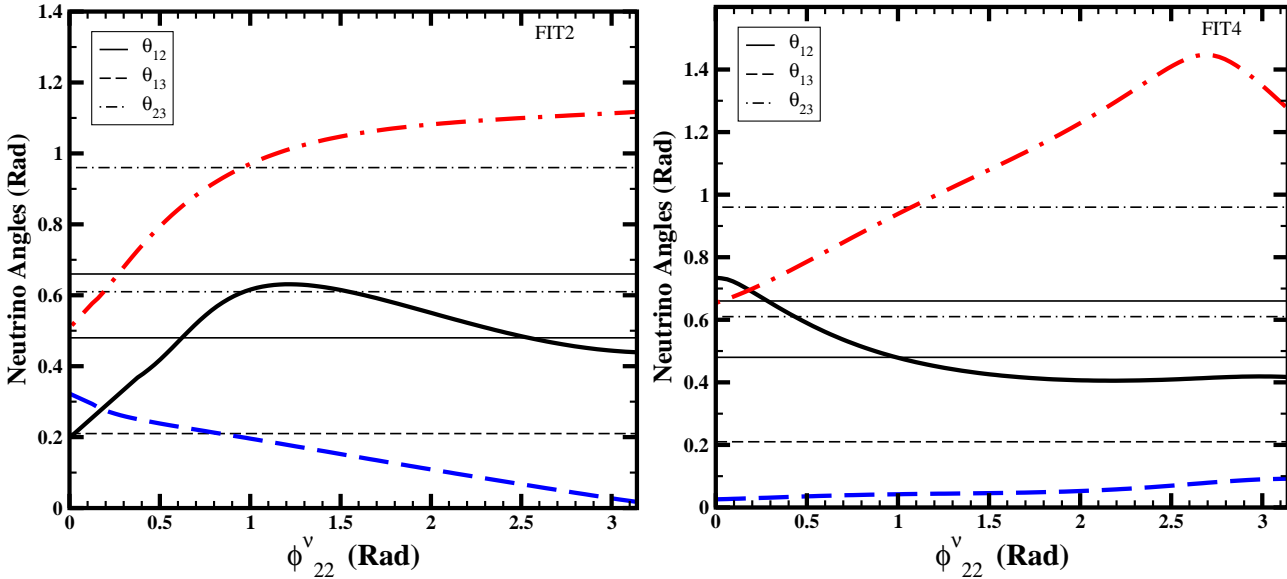


Figure 4: The neutrino mixing angles $\theta_{23,12,13}$ in various $SU(5)$ models, as functions of the phase $\phi_{22}^\nu \equiv \text{Arg}(a_{22}^\nu)$. The textures correspond to Fits 2 and 4 of [32] for the values of the coefficients a_{ij} in tables 5 and 6. The experimental limits on the three neutrino angles are denoted by horizontal lines.

As in the first model example, the changes induced by altering the numerical values of the coefficients a_{ij} affect the coefficients in the expansions of the mass matrices, but not the powers

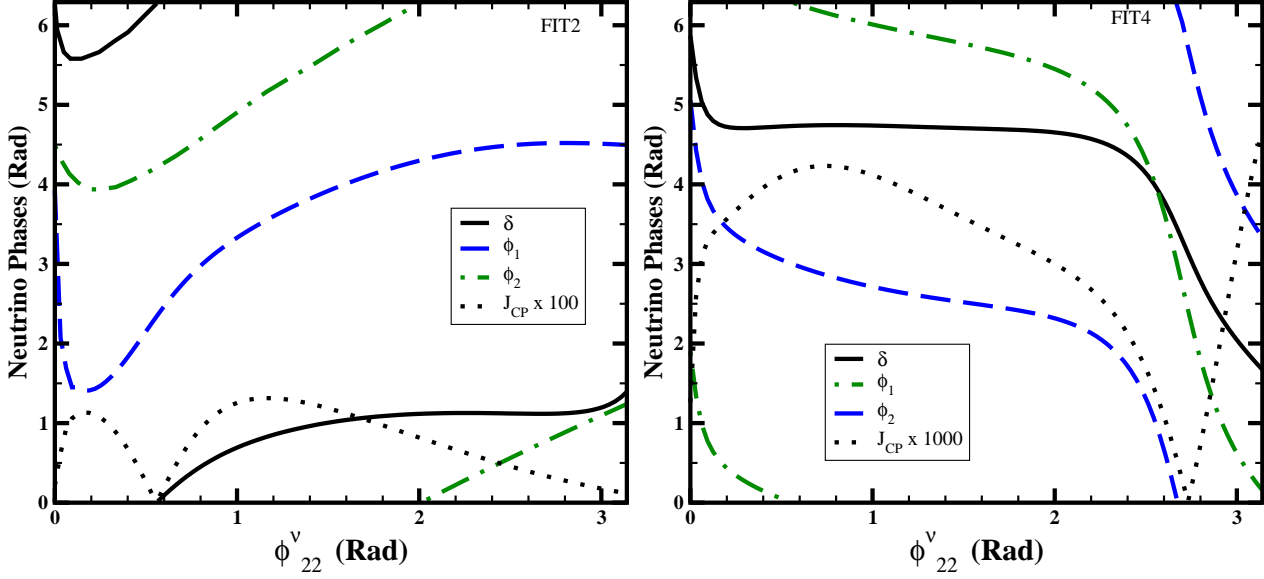


Figure 5: The neutrino phases and values of the CP-violating Jarlskog invariant J_{CP} as functions of the phase $\phi_{22}^v \equiv \text{Arg}(a_{22}^v)$ for Fit 2 and Fit 4, respectively.

Case	ϵ	σ	n_1
Fit 2	0.2	19/2	0
Fit 4	0.19	0.5	0

Table 4: Parameter values obtained for Fits 2 and 4 of [32], corresponding to the textures of eqns. (9.2, 9.3, 9.4) of that paper. The values are specified at the GUT scale, the n_i stand for the flavour charges of the right-handed neutrinos and σ is the flavour charge of the singlet field that, through its vev, generates the right-handed neutrino mass hierarchies.

	Fit 2 of [32]
Charged leptons	$a_{12}^e = 0.55, a_{21}^e = -0.6, a_{22}^e = 2, a_{23}^e = -0.7e^{i\pi/4}, a_{32}^e = 1.5, a_{33}^e = 1.4$
m_D^v	$a_{12}^v = .9, a_{22}^v = 2e^{i\pi/2}, a_{23}^v = 0.5$
M_{RR}	$a_{11}^N = 1.1, a_{12}^N = 1.2, a_{13}^N = 1.2, a_{22}^N = 2, a_{33}^N = 0.45$

Table 5: Choice of coefficients to reproduce the fermion observables for Fit 2 of [32]. Coefficients not appearing in the Table are set to unity.

	Fit 4 of [32]
Charged leptons	$a_{13}^e = 0.8, a_{22}^e = -2, a_{23}^e = 0.8e^{i\pi/5}, a_{33}^e = 1.1,$
m_D^v	$a_{13}^v = 0.5, a_{22}^v = 0.7e^{i\pi/4}, a_{32}^v = 1.9, a_{33}^v = 0.7$
M_{RR}	$a_{22}^N = 2, a_{23}^N = 0.65, a_{33}^N = 1.4$

Table 6: Choice of coefficients to reproduce the fermion data for Fit 4 of [32]. Coefficients not appearing in the table are set to unity.

Observables	Series Expansions	Numerical Values
m_{ν_3} (eV)	$-0.055 + 0.0071\epsilon^{-3/2} + 0.0084\epsilon^{-5/4}$	0.05(-0.055)
m_{ν_1}/m_{ν_3}	$2.21\epsilon^2 + 0.12\epsilon^{5/2} - 0.051\epsilon^{11/4}$	0.16(0.09)
m_{ν_2}/m_{ν_3}	$4.13\epsilon^{3/2} - 0.29\epsilon^2 - 13.82\epsilon^{9/4}$	0.20(0.37)
M_1/M_3	$0.82\epsilon - 0.98\epsilon^{5/4} + 0.55\epsilon^{3/2}$	0.06(0.16)
M_2/M_3	$0.63\epsilon^{1/4} - 1.49\epsilon^{1/2} + 1.73\epsilon^{3/4}$	0.12(0.42)
$m_{\nu_{ee}}$ (eV)	$0.017\epsilon^{4/3} + 0.04\epsilon^{5/3} - 0.85\epsilon^2$	0.0042(0.002)
θ_{23}	$1.08 + 0.17\epsilon^{3/4} - 0.012\epsilon^{4/3}$	0.91(1.13)
θ_{12}	$0.153\epsilon^{1/4} - 0.10\epsilon^{2/3} + 0.066\epsilon^{3/4}$	0.56(0.10)
θ_{13}	$0.21\epsilon^{2/3} + 0.25\epsilon + 0.0004\epsilon^{4/3}$	0.21(0.07)
δ	$-.45 + 0.059\epsilon^{1/3} - 0.31\epsilon^{5/12}$	0.43(-0.45)
J_{CP}	$0.0029\epsilon^{11/12} + 0.003\epsilon^{5/4} + 0.0009\epsilon^{17/12}$	0.0088(0.00066)
ϕ_1	$2.13 + 0.23\epsilon^{1/3} - 0.63\epsilon^{5/12}$	2.94 (2.13)
ϕ_2	$2.04 + 0.23\epsilon^{1/3} - 1.25\epsilon^{5/12}$	4.6 (2.03)
ϵ_1	$0.044\epsilon^{3/2} - 0.079\epsilon^{7/4} - 0.001\epsilon^{9/4}$	0.00046(0.0039)
ϵ_2	$0.00046\epsilon^{3/4} + 0.0085\epsilon + 0.07\epsilon^{5/4}$	0.0007(0.00014)
ϵ_3	$0.00005\epsilon - 0.06\epsilon^{5/4} + 0.2\epsilon^{3/2}$	0.0003(0.000001)
$\eta_B \times \Delta$	—	$1.18 \times 10^{-7} (3.11 \times 10^{-7})$
$\frac{16\pi^2}{\kappa} \times m_{\tilde{L}_{12}}^2$	$0.11\epsilon^{2/3} + 0.023\epsilon^{11/12} - 2.64\epsilon$	0.44(0.037)
$BR(\mu \rightarrow e\gamma)$	—	$8.5 \times 10^{-12} (6.1 \times 10^{-14})$
$\frac{16\pi^2}{\kappa} \times m_{\tilde{L}_{13}}^2$	$0.057\epsilon^{2/3} + 0.012\epsilon^{11/12} - 0.58\epsilon$	0.11(0.02)
$BR(\tau \rightarrow e\gamma)$	—	$5.95 \times 10^{-13} (1.74 \times 10^{-14})$
$\frac{16\pi^2}{\kappa} \times m_{\tilde{L}_{23}}^2$	$0.24 + 0.05\epsilon^{1/4} + 0.002\epsilon^{1/2}$	0.34 (0.24)
$BR(\tau \rightarrow \mu\gamma)$	—	$5.1 \times 10^{-12} (2.6 \times 10^{-12})$

Table 7: Values of observables predicted by Fit 2 of [32], for $\tan\beta = 2.04$. The rate of convergence of each expansion in ϵ can be judged from the relative magnitudes of the expansion coefficients and by comparing the exact numerical values of the observables with those obtained by keeping only the first term in each expansion (in parenthesis).

Observables	Series Expansions	Numerical Values
m_{ν_3} (eV)	$-0.054\epsilon + 0.024\epsilon^{-1/2} + 0.02\epsilon^{-3/8}$	0.05(-0.054)
m_{ν_1}/m_{ν_3}	$0.26\epsilon^{3/2} + 0.50\epsilon^{7/4} + 0.34\epsilon^{15/8}$	0.069(0.022)
m_{ν_2}/m_{ν_3}	$1.04\epsilon^{1/2} - 1.94\epsilon^{3/4} + 1.24\epsilon^{7/8}$	0.21(0.45)
M_1/M_3	$0.046 - 0.04\epsilon^{1/8} - 0.003\epsilon^{1/4}$	0.034(0.046)
M_2/M_3	$0.95 - 1.64\epsilon^{1/8} + 1.41\epsilon^{1/4}$	0.15(0.95)
$m_{\nu_{ee}}$ (eV)	$0.026\epsilon^{7/4} + 0.15\epsilon^2 + 0.05\epsilon^{17/8}$	0.0027(0.0014)
θ_{23}	$0.90 - 0.027\epsilon^{3/8} - 0.53\epsilon^{1/2}$	0.87(0.66)
θ_{12}	$0.5\epsilon^{1/2} + 0.94\epsilon^{3/4} + 0.026\epsilon^{7/8}$	0.53(0.22)
θ_{13}	$0.54\epsilon - 0.27\epsilon^{11/8} - 0.88\epsilon^{3/2}$	0.04(0.10)
δ	$2.56 - 0.025\epsilon^{1/4} + 0.03\epsilon^{3/8}$	4.87(2.56)
J_{CP}	$0.036\epsilon^{3/2} + 0.068\epsilon^{7/4} - 0.017\epsilon^{15/8}$	0.004(0.003)
ϕ_1	$5.19 - 0.074\epsilon^{1/4} + 0.096\epsilon^{3/8}$	6.17(5.20)
ϕ_2	$2.056 + 0.025\epsilon^{1/4} + 0.096\epsilon^{3/8}$	2.91(2.06)
ϵ_1	$0.000085\epsilon^{3/8} + 0.00017\epsilon^{1/2} - 0.00013\epsilon^{5/8}$	0.00087(0.000046)
ϵ_2	$0.0013\epsilon^{3/8} - 0.0012\epsilon^{1/2} + 0.00053\epsilon^{5/8}$	0.0012(0.00071)
ϵ_3	$0.0014\epsilon^{3/8} + 0.0013\epsilon^{1/2} + 0.0006\epsilon^{5/8}$	0.0002(0.00074)
$\eta_B \times \Delta$	—	$1.62 \times 10^{-7} (1.03 \times 10^{-7})$
$\frac{16\pi^2}{\kappa} \times m_{L12}^2$	$0.17\epsilon^{5/8} + 0.00024\epsilon^{3/4} - 0.046\epsilon^{7/8}$	0.05(0.06)
$BR(\mu \rightarrow e\gamma)$	—	$7.8 \times 10^{-13} (1.04 \times 10^{-12})$
$\frac{16\pi^2}{\kappa} \times m_{L13}^2$	$0.32\epsilon^{5/8} + 0.0066\epsilon^{3/4} - 0.062\epsilon^{7/8}$	0.16(0.12)
$BR(\tau \rightarrow e\gamma)$	—	$7.9 \times 10^{-12} (3.9 \times 10^{-12})$
$\frac{16\pi^2}{\kappa} \times m_{L23}^2$	$0.24 + 0.12\epsilon^{1/8} + 0.035\epsilon^{1/4}$	0.48(0.24)
$BR(\tau \rightarrow \mu\gamma)$	—	$6.6 \times 10^{-11} (1.7 \times 10^{-11})$

Table 8: Values of observables predicted by Fit 4 of [32], for $\tan\beta = 5.15$. The level of convergence of each expansion in ϵ can be judged from the relative magnitudes of the expansion coefficients and by comparing the exact numerical values of the observables with that obtained by keeping only the three first terms in each expansion (shown in parenthesis).

of ϵ . However, when varying the absolute values and the phases of the coefficients a_{ij}^ϵ , the numerical values of the observables are generally affected. We note the following points in connection with these two examples.

(i) In both fits, the dominant terms in the expansions generally agree only in order of magnitude with the exact numerical values, for the values of ϵ required to reproduce the correct fermion mass hierarchies. The leading term in many expansions is of order $z \equiv \epsilon^{1/8}$, and yields good numerical results only when $z \sim 0.5 - 0.75$ (i.e., $\epsilon \sim 0.05 - 0.1$). This slow convergence leads to the numerical instabilities that are evident in many observables, for example in J_{CP} , as shown in Fig. 3. These instabilities may be introduced by combinations of the following: (a) the powers of ϵ in the series are often very close to each other (e.g., $a\epsilon^{3/8} + b\epsilon^{4/8} + c\epsilon^{5/8}$), and (b) the relative signs of the terms in the expansions may change with the choice of a_{ij} .

(ii) The model predictions for θ_{23} is $\mathcal{O}(1)$, and that for θ_{12} is suppressed only by $\mathcal{O}(\epsilon^{1/4})$. As seen in Fig. 4, the numerical values of these angles are reasonable for ϕ_{22}' in Fit 2, in which case the prediction for θ_{13} is close to the present experimental upper limit, even though parametrically it is suppressed by $\mathcal{O}(\epsilon^{2/3})$. In the case of Fit 4, the values of $\theta_{23,12}$ are reasonable for $0.3 < \phi_{22}' < 1$, but θ_{13} is always considerably below the present experimental upper limit.

(iii) The complex phases δ and $\phi_{1,2}$ are $\mathcal{O}(1)$ in both fits, but vary widely with ϕ_{22}' , as seen in Fig. 5.

(iv) Observable CP-violation is to be expected in neutrino oscillations, although the Jarlskog invariant J_{CP} is significantly smaller than in the case of large $\tan\beta$, as also seen in Fig. 5, particularly for Fit 4. In this later case, there is a rather good agreement between the numerical value and the dominant terms in the expansion.

(v) Both Fit 2 and Fit 4 may accommodate successful leptogenesis, and also lead to lepton flavour violation that is close to the present experimental upper limits. Values of η_b in the range of eq. (17) would be obtained with the values presented in Table 7 and Table 8 if the dilution factor $\Delta \sim 200$. As we discussed in the previous subsection, a global scaling factor f_s for m_D^ν and the corresponding rescaling of M_{RR} would imply a modification of the leptogenesis (and lepton-flavour violation) predictions. We find that a factor $f_s \sim 0.06 - 0.07$ would predict η_B in the range of eq. (17) with $\Delta \sim 1$ and $M_3 \sim 10^{12}$ GeV. However, this would imply a reduction of about two orders of magnitude in the predictions for charged-lepton-flavor violation.

(vi) The numerical results shown in Fig. 4 further demonstrate the inter-correlations between the different physical parameters, indicating how the experimental limits on neutrino masses constrain the allowed range for the angles, phases, and J_{CP} . We see that, even for the same GUT group and range of $\tan\beta$, the relations between the observables display certain differences, reflecting among others the role of the coefficients in obtaining viable solutions in these schemes.

3.4 Flipped SU(5) Model

In the case of the flipped SU(5) GUT model, the fields Q_i, d_i^c and ν_i^c of each family belong to a 10 representation of SU(5), the u_i^c and L_i belong to $\bar{5}$ representations, and the e_i^c fields belong to singlet representations of SU(5). Thus the correlations between the U(1) charges of the different matter fields are different from those in conventional SU(5). These particle

assignments imply a symmetric down-quark mass matrix, whereas the structure of the up-quark mass matrix depends on the charges of the right-handed quarks. However, as these are the same as the charges of the left-handed leptons, the up-quark mass matrix is constrained by the need to generate large mixing for atmospheric neutrinos.

The simplest example that matches the charged-fermion mass hierarchies (adjusting coefficients so as to match the experimental value of V_{cb}) is [16]

$$M_{down} \propto \begin{pmatrix} \bar{\epsilon}^8 & \bar{\epsilon}^3 & \bar{\epsilon}^4 \\ \bar{\epsilon}^3 & \bar{\epsilon}^2 & \bar{\epsilon} \\ \bar{\epsilon}^4 & \bar{\epsilon} & 1 \end{pmatrix}, M_{up} \propto \begin{pmatrix} \epsilon^{|-4+y|} & \epsilon^4 & \epsilon^4 \\ \epsilon^{|1+y|} & \epsilon & \epsilon \\ \epsilon^{|y|} & 1 & 1 \end{pmatrix}, \quad (33)$$

$$M_\ell \propto \begin{pmatrix} \bar{\epsilon}^{|a+y|} & \bar{\epsilon}^{|b+y|} & \bar{\epsilon}^{|y|} \\ \bar{\epsilon}^{|a|} & \bar{\epsilon}^{|b|} & 1 \\ \bar{\epsilon}^{|a|} & \bar{\epsilon}^{|b|} & 1 \end{pmatrix}, M_\nu^D \propto \begin{pmatrix} \epsilon^{|-4+y|} & \epsilon^{|1+y|} & \epsilon^{|y|} \\ \epsilon^4 & \epsilon & 1 \\ \epsilon^4 & \epsilon & 1 \end{pmatrix}. \quad (34)$$

Once again, the form of the heavy Majorana mass matrix depends on the charge of the field Σ . For instance, for $\sigma = 0$, it will be similar in structure to the down-quark mass matrix. The contribution from the up-quark sector to V_{cb} is generically small in this model, leading to $V_{cb} \simeq \sqrt{m_s/m_b}$. (indeed, for the up-type quark hierarchies, it turns out that $\bar{\epsilon} \approx 0.2$, $\epsilon \sim \bar{\epsilon}^4$ and $|y| \sim 2$). This is too large, and requires a significant adjustment of the $\mathcal{O}(1)$ coefficients.

However, the problem with the large value of V_{cb} can be avoided by combining flipped SU(5) with a non-Abelian flavour group, or by adding a second singlet field with different transformation properties under the flavour group. In that way, one could obtain solutions similar to those of [18], with

$$M_{down} \propto \begin{pmatrix} \bar{\epsilon}^8 & \bar{\epsilon}^3 & \bar{\epsilon}^4 \\ \bar{\epsilon}^3 & \bar{\epsilon}^2 & \bar{\epsilon}^2 \\ \bar{\epsilon}^4 & \bar{\epsilon}^2 & 1 \end{pmatrix}. \quad (35)$$

However, even after overcoming this obstacle, it is very difficult to obtain naturally viable solutions: if $\epsilon \sim \bar{\epsilon}^4$, the Dirac-mass hierarchies turn out to be too large to generate interesting solutions. Of course, the fact that the see-saw mechanism is hard to implement does not mean that an appropriate m_{eff} could not be generated by alternative mechanisms. However, the symmetries require that

$$m_{eff} \propto \begin{pmatrix} \bar{\epsilon}^{|2y|} & \bar{\epsilon}^{|y|} & \bar{\epsilon}^{|y|} \\ \bar{\epsilon}^{|y|} & 1 & 1 \\ \bar{\epsilon}^{|y|} & 1 & 1 \end{pmatrix}$$

indicating that, unlike in conventional SU(5), it is difficult to generate large solar mixing.

As in the case of conventional SU(5), one could either (i) study the most generic cases with half-integer charges, requiring the (3,3) flavour charges to be non-zero, and using the see-saw conditions to obtain large mixing for the solar neutrinos, or (ii) add further fields and flavour groups. However, any departure from the simple structure described so far introduces significant model dependence, and results in a loss of predictivity, unless this additional structure is predicted (and constrained) by concrete theoretical considerations. In the subsection that follows, we discuss what may be the most natural way to proceed, if one believes in the existence of an underlying string theory.

3.5 String-Derived Flipped SU(5) Models

So far, we have been discussing models based on a single U(1) flavour symmetry, and with only one field θ whose vev provides a single expansion parameter in the mass matrices. However, in realistic models this need not be the case. On the contrary, one may expect several fields to be involved in the generation of mass terms, while additional flavour symmetries may be relevant. While this seems to limit predictivity, in models based on an underlying string theory, the string symmetries (translated into selection rules) impose strong constraints on the mass and mixing matrices.

In the previous sections we observed that there is significant model-dependence in the results, and that the values of certain coefficients must be in specific ranges in order to give viable solutions. Optimally, we would like to understand these values from prior principles. In a realistic model, they could be related to the vacuum expectation values of fields that are constrained, for example, by considerations on flat directions.

In specific string-derived models, due to the string selection rules, several texture zeros are generated in the matrices, and these could in principle lead to strong constraints on certain observables. Indeed, the constraints are so strong that one could expect that it might be difficult to generate the required entries that fully reproduce the observed fermion patterns. Nevertheless, it was found in [36, 37] that it is possible to accommodate all data in a natural and generic way within a flipped SU(5) \times U(1) string model [38]. Relevant aspects of this model are reviewed in Appendix II: the theory contains many singlet fields, and the mass matrices depend on the subset of them that get non-zero vev's, i.e., on the choice of flat directions in the effective potential.

The flat directions and the quark masses and mixings for this model have been studied in [36], where it was found that

$$M_D = \begin{pmatrix} 0 & \Delta_2 \Delta_3^2 \bar{\Phi}_{23} & \Delta_5 \Delta_3 \bar{\phi}_3 \\ \Delta_2 \Delta_3 \bar{\Phi}_{23} & (\bar{\phi}_3^2 + \bar{\phi}_4^2) & \Delta_2 \Delta_5 \bar{\phi}_4 \\ \Delta_5 \Delta_3 \bar{\phi}_3 & \Delta_2 \Delta_5 \bar{\phi}_4 & 1 \end{pmatrix}, \quad M_U = \begin{pmatrix} 0 & 0 & \Delta_5 \Delta_3 \bar{\phi}_3 \\ 0 & \bar{\phi}_4 & \Delta_2 \Delta_5 \bar{\phi}_4 \\ 0 & \Delta_2 \Delta_5 & 1 \end{pmatrix}. \quad (36)$$

As already remarked, the relevant field definitions are given in Appendix II. For instance, $\Delta_2 \Delta_5$ is a combination of hidden-sector fields that transform as sextets under SO(6).

The lepton mass matrices were studied in [37], where it was shown that:

$$m_\ell \propto \begin{pmatrix} \bar{\phi}_4^2 & \Delta_2 \Delta_5 \bar{\phi}_3^2 & 0 \\ 0 & \bar{\phi}_3^2 & 0 \\ 0 & 0 & 1 \end{pmatrix} \equiv \begin{pmatrix} f^2 & xu^2 & 0 \\ 0 & u^2 & 0 \\ 0 & 0 & 1 \end{pmatrix}, \quad (37)$$

$$m_\nu^D \propto \begin{pmatrix} \Delta_2 \Delta_5 \bar{\phi}_4 & 1 & 0 \\ \bar{\phi}_4 & \Delta_2 \Delta_5 & 0 \\ 0 & 0 & F_1 \end{pmatrix} \equiv \begin{pmatrix} fx & 1 & 0 \\ f & x & 0 \\ 0 & 0 & F_1 \end{pmatrix}, \quad (38)$$

$$M_{\nu_R} \propto \begin{pmatrix} \bar{F}_5 \bar{F}_5 \bar{\phi}_4 \phi_3 & \bar{F}_5 \bar{F}_5 \Delta_2 \Delta_5 \phi_3 & 0 \\ \bar{F}_5 \bar{F}_5 \Delta_2 \Delta_5 \phi_3 & 0 & \bar{F}_5 \bar{\Phi}_{31} \bar{\Phi}_{31} \bar{\phi}_4 \phi_2 \\ 0 & \bar{F}_5 \bar{\Phi}_{31} \bar{\Phi}_{31} \bar{\phi}_4 \phi_2 & \Delta_2 \Delta_5 \bar{\Phi}_{23} T_2 T_5 \end{pmatrix} \equiv \begin{pmatrix} fry^2 & 2rxy^2 & 0 \\ 2rxy^2 & 0 & bfy \\ 0 & bfy & ctx \end{pmatrix}, \quad (39)$$

where

$$y \equiv \bar{F}_5, r \equiv \phi_3, b \equiv \bar{\Phi}_{31}\Phi_{31}\phi_2, c \equiv \bar{\Phi}_{23}, \bar{\phi}_3 \equiv u. \quad (40)$$

Note that these matrices are given in the flipped SU(5) field basis. However it is easy to pass to the weak interaction eigenstates by an appropriate rotation. For instance, the weak-interaction eigenstates for the light neutrinos have the following assignments:

$$\nu_e \rightarrow \bar{f}_5 - \mathcal{O}(\Delta_2\Delta_5)\bar{f}_2, \quad \nu_\mu \rightarrow \bar{f}_2 + \mathcal{O}(\Delta_2\Delta_5)\bar{f}_5, \quad \nu_\tau \rightarrow \bar{f}_1, \quad (41)$$

while the flipped SU(5) basis $(\bar{f}_5, \bar{f}_2, \bar{f}_1)$ is related to (41) by the rotation

$$V_{\ell_L}^m = \begin{pmatrix} 1 - \frac{1}{2}(\Delta_2\Delta_5)^2 & \Delta_2\Delta_5 & 0 \\ -\Delta_2\Delta_5 & 1 - \frac{1}{2}(\Delta_2\Delta_5)^2 & 0 \\ 0 & 0 & 1 \end{pmatrix}. \quad (42)$$

The forms of the mass matrices depend on the various field vev's. The analysis of quark masses pointed towards $x = \Delta_2\Delta_5 = \mathcal{O}(1)$ (and potentially large solar mixing, already from the charged-lepton sector), as well as a rather suppressed value of $f = \bar{\phi}_4 \ll 1$ (since $V_{cb} \approx \Delta_2\Delta_5\bar{\phi}_4$). Moreover, from the analysis of flat directions [36], it was concluded that $\bar{\Phi}_{31}\bar{\Phi}_{23} = \mathcal{O}(1)$ is large. In addition, the flatness conditions [36] relate $\bar{\Phi}_{31}, \Phi_{31}$ and ϕ_2 , and can be satisfied even if all the vev's are large, as long as $\bar{\Phi}_{31}\Phi_{31}$ and $\bar{\Phi}_{23}\Phi_{23}$ are not very close to unity. As for the decuplets that break the gauge group down to the Standard Model, we know that the vev's should be $\approx M_{GUT}/M_s$. In weakly-coupled string constructions, this ratio is ≈ 0.01 . However, the strong-coupling limit of M theory offers the possibility that the GUT and the string scales can coincide, in which case the vev's could be of order unity.

The 2×2 form of the charged-lepton mass matrix in fact puts severe constraints on the fields involved. On the other hand, flatness conditions and quark masses do not give any information on the vev of the product T_2T_5 . However, this combination is to some extent constrained by the requirements for the light neutrino masses [37]. Finally, the field ϕ_3 is the one for which we seem to know least and we can consider two extreme possibilities: a very large value $\mathcal{O}(1)$ and a very small value. For large ϕ_3 , if $\bar{\phi}_4 \approx \bar{F}_5, F_1$ as would be expected in weak-coupling unification schemes, the entries of m_{eff} are all of the same order of magnitude, and large $\nu_\mu - \nu_e$ and $\nu_\mu - \nu_\tau$ mixings are naturally generated via the neutrino mixing matrix.

Charged-lepton mass hierarchies pose severe constraints on the model parameters. From (37) we get

$$m_e/m_\mu \sim \frac{f^2}{u^2(1+x^2)}, \quad (43)$$

while f and x are also constrained from the quark masses, by

$$m_c/m_t \sim f \times \mathcal{O}(1), \quad (44)$$

$$V_{cb} \sim xf \sim 0.044. \quad (45)$$

Therefore, if f is $\mathcal{O}(0.01)$, x can be $\mathcal{O}(1)$ while the charged leptons mass ratio can be satisfied with u of $\mathcal{O}(0.1)$.

The charged-lepton mixing matrix V_e is obtained by the diagonalization of m_ℓ in the weak-interaction basis:

$$V_e^T (V_{\ell L}^m)^T m_\ell m_\ell^\dagger (V_{\ell L}^m)^* V_e^* = \text{Diag}(m_e^2, m_\mu^2, m_\tau^2). \quad (46)$$

We parametrize the product of these two rotations by defining:

$$Q_e = V_e V_{\ell L}^m \sim \begin{pmatrix} 1/N & g/N & 0 \\ -g/N & 1/N & 0 \\ 0 & 0 & 1 \end{pmatrix}, \quad (47)$$

where g is a mixing parameter to be determined by the neutrino mass matrix, and N is a normalization factor for the sector 1-2: $N = 1/(1 + |g|^2)^{1/2}$.

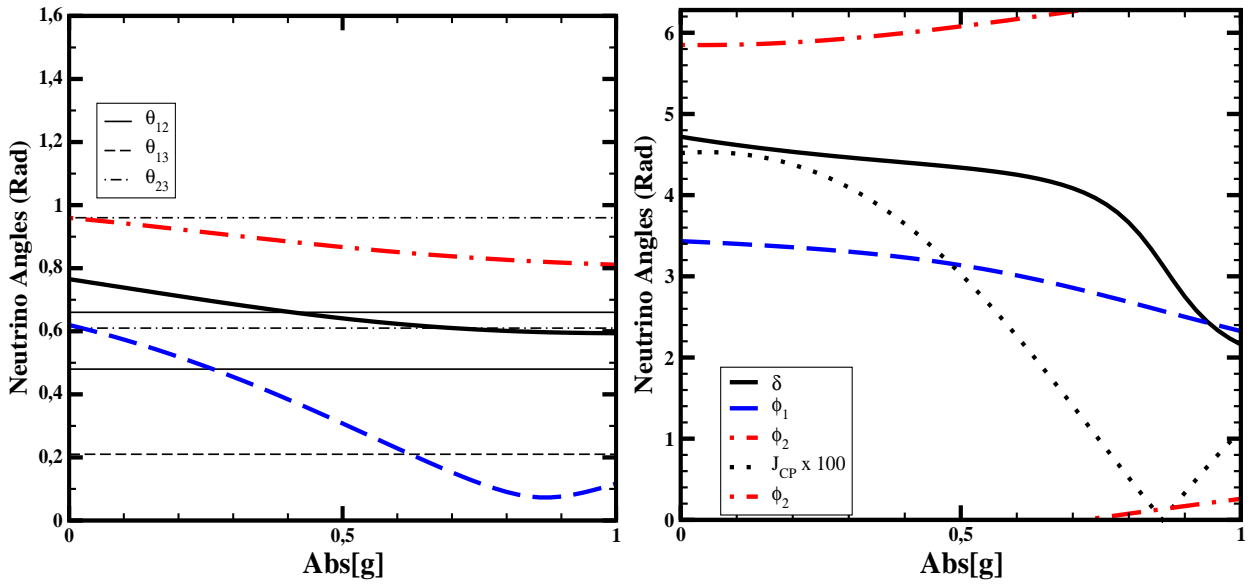


Figure 6: The neutrino mixing angles (left) and the phases and value of the CP-violating Jarlskog invariant J_{CP} (right), as functions of the absolute value of g . The experimental limits on the three neutrino angles are denoted by horizontal lines.

Passing finally to the neutrino mass matrix, we see the following. In the basis where the charged-lepton masses are diagonal, (*i.e.* $m_\nu^D \rightarrow Q_e^T \cdot m_\nu^D$), the vev's for the remaining fields m_ν^D and $M_{\nu R}$ enter in m_{eff} as combinations:

$$m_{eff} \propto \begin{pmatrix} (G_{11} + \mathbf{p} \cdot \mathbf{H}_{11})/N^2 & (G_{12} + \mathbf{p} \cdot \mathbf{H}_{12})/N^2 & \mathbf{q} \cdot (1 + gx - 2x^2)/N \\ (G_{12} + \mathbf{p} \cdot \mathbf{H}_{12})/N^2 & (G_{22} + \mathbf{p} \cdot \mathbf{H}_{22})/N^2 & -\mathbf{q} \cdot (x - g(1 - 2x^2))/N \\ \mathbf{q} \cdot (1 + gx - 2x^2)/N & -\mathbf{q} \cdot (x - g(1 - 2x^2))/N & 4\mathbf{q}^2 \cdot x^2 \end{pmatrix}. \quad (48)$$

Here, \mathbf{p} , \mathbf{q} are combinations of vev's defined as:

$$\mathbf{p} = \frac{\mathbf{c} \cdot \mathbf{r} \cdot \mathbf{t}}{b^2 \cdot f^3}, \mathbf{q} = \frac{\mathbf{y} \cdot \mathbf{f}_1 \cdot \mathbf{r}}{b \cdot f^2}, \quad (49)$$

while the functions $G_{ij}(x, g)$, $H_{ij}(x, g)$, are of $\mathcal{O}(1)$:

$$G_{11}(x, g) = g^2 - 2gx + x^2,$$

$$\begin{aligned}
G_{12}(x, g) &= x - g^2x + g(-1 + x^2), \\
G_{22}(x, g) &= 1 + 2gx + g^2x^2, \\
H_{11}(x, g) &= 3g^2x^3 + x(-1 + 4x^2) - 2gx(x + 2x^3), \\
H_{12}(x, g) &= gx(-1 + x^2) + x(x + 2x^3) - g^2x(x + 2x^3), \\
H_{22}(x, g) &= 3x^3 + g^2x(-1 + 4x^2) + 2gx(x + 2x^3).
\end{aligned} \tag{50}$$

The phase of \mathbf{q} can be eliminated with a rotation $q_3 \cdot m_{eff} \cdot q_3$, where $q_3 = \text{diag}(1, 1, \text{Arg}(q)/2)$. The neutrino data can be fit by choosing suitably the parameters \mathbf{p} , \mathbf{q} , g and x . The results presented in Table 9 correspond to following choice of parameters:

$$x = 0.8 \cdot e^{0.3i}, \quad g = 0.7 \cdot e^{-0.94i}, \quad \mathbf{p} = 0.43 \cdot e^{2.2i}, \quad \mathbf{q} = 0.25, \tag{51}$$

while in Fig. 6 we vary the value of $|g|$ while keeping constant the rest of the parameters.

To estimate the values of the observables that involve the right-handed neutrinos, we need the individual values of the vev's contained in \mathbf{p} , \mathbf{q} . Since, b, c, r are $\mathcal{O}(1)$, $t \sim f^3$ and also $y \sim F_1 \sim f$. In order to provide some numerical values we can make the assignment $y = F_1 = t^{1/3} = |f| = 0.01$. Then, from the values of \mathbf{p} , \mathbf{q} we can get:

$$|r/b| = 1/4, \quad |c/b| = 1.84. \tag{52}$$

Despite the phase dependence of $M_{\nu R}$ being rather complex since all the vev's contain phases, these appear on the observables $\epsilon_{1,2}$ and $\text{BR}(\mu \rightarrow e\gamma)$ in the same combination as the phase of \mathbf{p} . For field vev's chosen as above, the matrix $M_{\nu R}$ in (39) contains two almost degenerate eigenvalues $M_{1,2} \sim |(M_{\nu R})_{12}^2 + (M_{\nu R})_{23}^2|^{1/2}$. The predictions of the string-derived flipped SU(5) model for the neutrino masses, mixing angles, CP and charged-lepton flavour violation are shown in Table 9.

The following are some notable features.

(i) Since the vev's are fixed in the string-derived flipped SU(5) model, there is no auxiliary expansion parameter, as in the previous SU(5) models. However, it is interesting to study observables as a function of g , as shown in Fig. 6.

(ii) We see in Fig. 6 that θ_{23} is large and within the experimental range for all values of g , whereas θ_{12} lies within the allowed range for $|g| > 0.5$, and θ_{13} is acceptably small for $|g| > 0.6$ and may lie close to the experimental upper limit.

(iii) We also see in Fig. 6 that δ and the two low-energy Majorana phases are expected to be quite large.

(iv) We also see that J_{CP} may be quite large, though there is also the possibility that it might (be close to) vanish(ing).

(v) We see in Table 9 that leptogenesis is quite possible. Values of η_b in the range of eq. (17) with the values presented in Table 9 are consistent with a dilution factor $\Delta \sim 80$. In this case, we find that a global scaling factor $f_s \sim 0.11$ on m_D^{ν} would predict η_B in the range of eq. (17) with $\Delta \sim 1$ and $M_3 \sim 10^{12}$ GeV. Such a scaling would decrease the prediction for $\text{BR}(\mu \rightarrow e\gamma)$ by two orders of magnitude, making it compatible with the experimental bound for a lower range of supersymmetric masses.

Observables	Numerical Values
m_{ν_3} (eV)	0.056
m_{ν_1}/m_{ν_3}	0.008
m_{ν_2}/m_{ν_3}	0.17
M_1/M_3	1.4×10^{-4}
M_2/M_3	0.98
$m_{\nu_{ee}}$ (eV)	0.0027
θ_{23}	0.84
θ_{12}	0.61
θ_{13}	0.15
δ	4.1
J_{CP}	0.014
ϕ_1	2.86
ϕ_2	6.26
ϵ_1	1.5×10^{-7}
ϵ_2	3.1×10^{-3}
ϵ_3	3.2×10^{-3}
$\eta_B \times \Delta$	4.5×10^{-8}
$BR(\mu \rightarrow e\gamma) \times \frac{1}{(\tan\beta)^2}$	2.4×10^{-10}

Table 9: Values of observables predicted in the string-derived flipped $SU(5)$ model for the choice of parameters given in the text.

(vi) The values of Table 9 correspond to $M_3 = 10^{14}$ GeV. However, these imply a $BR(\mu \rightarrow e\gamma)$ above the experimental bound (unless the supersymmetry breaking masses become very large), due to $\mathcal{O}(1)$ entries in the Dirac neutrino mass matrix (38). Clearly, by lowering the heavy right-handed neutrino masses, and thus also the Dirac neutrino couplings, the rates are altered accordingly. For example, $M_3 = 5 \times 10^{12}$ GeV would yield $BR(\mu \rightarrow e\gamma) \sim 1.4 \cdot 10^{-12} \cdot \tan^2 \beta$, while $\epsilon_1 \sim \epsilon_2 \sim 1.5 \cdot 10^{-4}$. The expressions for $\epsilon_{1,2}$ and $BR(\mu \rightarrow e\gamma)$ contain Y_ν in a basis where M_{ν_R} is diagonal, so their values have the same phase dependence as in the 1-2 sector of m_{eff} . Hence, with the choice of parameters of (51), the results presented in Table 9 are independent of the individual phases of the parameters included in the definition of \mathbf{p} in (49).

(vii) On the contrary, due to the lack of mixing in the third generation in this model, τ decays are not observable in this case.

4 Conclusions

We have studied in this paper the predictions for CP and charged-lepton-number violation in different $SU(5)$ models, including a string version of flipped $SU(5)$. Because of the inter-correlations between the different neutrino observables, it was in each case possible to obtain quite specific predictions, which differ significantly between the models.

The general indications are that accessible rates for CP and charged-lepton-number violation are to be expected. However, due to the different expectations for the couplings and angles in the various models, the magnitudes of the observables may be quite different, even between models based on the same group. We note that θ_{13} may be close to the present experimental upper limit in some models, but much smaller in others. Also, the predictions for the Jarlskog invariant J_{CP} vary significantly. Among the most sensitive observables are those for charged-lepton-flavour violation and leptogenesis, and cases with a resonant enhancement of the expected lepton asymmetry for degenerate heavy Majorana neutrinos are particularly interesting.

It is crucial to keep in mind that the various models sometimes contain instabilities due to cancellations, to which the results may be sensitive. In principle, for cases such as the flipped SU(5) string model, we expect that the coefficients are to a good extent predicted by the vev's of the fields. However, one should not forget that there is a sum of non-renormalisable terms, implying that, if the higher-order terms involve fields with high vev's, they can effectively introduce multiplicative factors, particularly in the case of many fields. In principle, once some of the observables discussed here are measured, one may use the correlated data to refine the predictions with better knowledge of the possible ranges of coefficients and the level of tuning via sub-determinant cancellations. However, such an analysis is premature ahead of the corresponding measurements, and would go beyond the scope of this paper.

Appendix I: GUT Fits 2 and 4 of [32]

We give here the matrix parametrizations found in Fits 2 and 4, as used in the text.

Fit 2

$$\begin{aligned}
Y^u &= \begin{bmatrix} a_{11}^u \epsilon^{16} & a_{12}^u \epsilon^6 & a_{13}^u \epsilon^8 \\ a_{21}^u \epsilon^6 & a_{22}^u \epsilon^4 & a_{23}^u \epsilon^2 \\ a_{31}^u \epsilon^8 & a_{32}^u \epsilon^2 & a_{33}^u \end{bmatrix}, & Y^d &= \begin{bmatrix} a_{11}^d \epsilon^{31/2} & a_{12}^d \epsilon^{11/2} & a_{13}^d \epsilon^{11/2} \\ a_{21}^d \epsilon^{11/2} & a_{22}^d \epsilon^{9/2} & a_{23}^d \epsilon^{9/2} \\ a_{31}^d \epsilon^{15/2} & a_{32}^d \epsilon^{5/2} & a_{33}^d \epsilon^{5/2} \end{bmatrix}, \\
Y^e &= \begin{bmatrix} a_{11}^e \epsilon^{46/3} & a_{12}^e \epsilon^{16/3} & a_{13}^e \epsilon^{22/3} \\ a_{21}^e \epsilon^{16/3} & a_{22}^e \epsilon^{14/3} & a_{23}^e \epsilon^{8/3} \\ a_{31}^e \epsilon^{16/3} & a_{32}^e \epsilon^{14/3} & a_{33}^e \epsilon^{8/3} \end{bmatrix}, & Y^\nu &= \begin{bmatrix} a_{11}^\nu \epsilon^{|n_1+5|} & a_{12}^\nu \epsilon^{\frac{41}{8}} & a_{13}^\nu \epsilon^{\frac{11}{2}} \\ a_{21}^\nu \epsilon^{|n_1-5|} & a_{22}^\nu \epsilon^{\frac{39}{8}} & a_{23}^\nu \epsilon^{\frac{9}{2}} \\ a_{31}^\nu \epsilon^{|n_1-5|} & a_{32}^\nu \epsilon^{\frac{39}{8}} & a_{33}^\nu \epsilon^{\frac{9}{2}} \end{bmatrix}, \\
M_{RR} &= \begin{bmatrix} \epsilon^{|2n_1+\sigma|} & \epsilon^{|1/8+n_1+\sigma|} & \epsilon^{|1/2+n_1+\sigma|} \\ \cdot & a_{22}^N \epsilon^{|1/4+\sigma|} & \epsilon^{|5/8+\sigma|} \\ \cdot & \cdot & \epsilon^{|1+\sigma|} \end{bmatrix} \langle \Sigma \rangle. \tag{53}
\end{aligned}$$

Fit 4:

$$\begin{aligned}
Y^u &= \begin{bmatrix} a_{11}^u \epsilon^6 & a_{12}^u \epsilon^5 & a_{13}^u \epsilon^3 \\ a_{21}^u \epsilon^5 & a_{22}^u \epsilon^4 & a_{23}^u \epsilon^2 \\ a_{31}^u \epsilon^3 & a_{32}^u \epsilon^2 & a_{33}^u \end{bmatrix}, & Y^d &= \begin{bmatrix} a_{11}^d \epsilon^4 & a_{12}^d \epsilon^3 & a_{13}^d \epsilon^3 \\ a_{21}^d \epsilon^3 & a_{22}^d \epsilon^2 & a_{23}^d \epsilon^2 \\ a_{31}^d \epsilon & a_{32}^d & a_{33}^d \end{bmatrix} \epsilon^{|k_d|}, \\
Y^e &= \begin{bmatrix} a_{11}^e \epsilon^4 & a_{12}^e \epsilon^3 & a_{13}^e \\ a_{21}^e \epsilon^3 & a_{22}^e \epsilon^2 & a_{23}^e \\ a_{31}^e \epsilon^3 & a_{32}^e \epsilon^2 & a_{33}^e \end{bmatrix} \epsilon^{|k_e|}, & Y^\nu &= \begin{bmatrix} a_{11}^\nu \epsilon^{|n_1+1|} & a_{12}^\nu \epsilon^{5/8} & a_{13}^\nu \epsilon \\ a_{21}^\nu \epsilon^{|n_1-3/8|} & a_{22}^\nu \epsilon^{3/8} & a_{23}^\nu \\ a_{31}^\nu \epsilon^{|n_1|} & a_{32}^\nu \epsilon^{3/8} & a_{33}^\nu \end{bmatrix},
\end{aligned}$$

$$M_{RR} = \begin{bmatrix} \epsilon^{|2n_1+\sigma|} & \epsilon^{|-3/8+n_1+\sigma|} & \epsilon^{|n_1+\sigma|} \\ \cdot & a_{22}^N \epsilon^{|-3/4+\sigma|} & \epsilon^{|-3/8+\sigma|} \\ \cdot & \cdot & \epsilon^{|\sigma|} \end{bmatrix} \langle \Sigma \rangle. \quad (54)$$

Appendix II: Flipped SU(5) Particle Assignments

In this Appendix we tabulate for completeness the field assignment of the ‘realistic’ flipped SU(5) string model [38], as well as the basic conditions used in [36] to obtain consistent flatness conditions and acceptable Higgs masses.

$F_1(10, \frac{1}{2}, -\frac{1}{2}, 0, 0, 0)$	$\bar{f}_1(\bar{5}, -\frac{3}{2}, -\frac{1}{2}, 0, 0, 0)$	$\ell_1^c(1, \frac{5}{2}, -\frac{1}{2}, 0, 0, 0)$
$F_2(10, \frac{1}{2}, 0, -\frac{1}{2}, 0, 0)$	$\bar{f}_2(\bar{5}, -\frac{3}{2}, 0, -\frac{1}{2}, 0, 0)$	$\ell_2^c(1, \frac{5}{2}, 0, -\frac{1}{2}, 0, 0)$
$F_3(10, \frac{1}{2}, 0, 0, \frac{1}{2}, -\frac{1}{2})$	$\bar{f}_3(\bar{5}, -\frac{3}{2}, 0, 0, \frac{1}{2}, \frac{1}{2})$	$\ell_3^c(1, \frac{5}{2}, 0, 0, \frac{1}{2}, \frac{1}{2})$
$F_4(10, \frac{1}{2}, -\frac{1}{2}, 0, 0, 0)$	$f_4(5, \frac{3}{2}, \frac{1}{2}, 0, 0, 0)$	$\ell_4^c(1, -\frac{5}{2}, \frac{1}{2}, 0, 0, 0)$
$\bar{F}_5(\bar{10}, -\frac{1}{2}, 0, \frac{1}{2}, 0, 0)$	$\bar{f}_5(\bar{5}, -\frac{3}{2}, 0, -\frac{1}{2}, 0, 0)$	$\ell_5^c(1, \frac{5}{2}, 0, -\frac{1}{2}, 0, 0)$
$h_1(5, -1, 1, 0, 0, 0)$	$h_2(5, -1, 0, 1, 0, 0)$	$h_3(5, -1, 0, 0, 1, 0)$
$h_{45}(5, -1, -\frac{1}{2}, -\frac{1}{2}, 0, 0)$		
$\phi_{45}(1, 0, \frac{1}{2}, \frac{1}{2}, 1, 0)$	$\phi_+(1, 0, \frac{1}{2}, -\frac{1}{2}, 0, 1)$	$\phi_-(1, 0, \frac{1}{2}, -\frac{1}{2}, 0, -1)$
$\Phi_{23}(1, 0, 0, -1, 1, 0)$	$\Phi_{31}(1, 0, 1, 0, -1, 0)$	$\Phi_{12}(1, 0, -1, 1, 0, 0)$
$\phi(1, 0, \frac{1}{2}, -\frac{1}{2}, 0, 0)$	$\Phi(1, 0, 0, 0, 0, 0)$	
$\Delta_1(0, 1, 6, 0, -\frac{1}{2}, \frac{1}{2}, 0)$	$\Delta_2(0, 1, 6, -\frac{1}{2}, 0, \frac{1}{2}, 0)$	$\Delta_3(0, 1, 6, -\frac{1}{2}, -\frac{1}{2}, 0, \frac{1}{2})$
$\Delta_4(0, 1, 6, 0, -\frac{1}{2}, \frac{1}{2}, 0)$	$\Delta_5(0, 1, 6, \frac{1}{2}, 0, -\frac{1}{2}, 0)$	
$T_1(0, 10, 1, 0, -\frac{1}{2}, \frac{1}{2}, 0)$	$T_2(0, 10, 1, -\frac{1}{2}, 0, \frac{1}{2}, 0)$	$T_3(0, 10, 1, -\frac{1}{2}, -\frac{1}{2}, 0, \frac{1}{2})$
$T_4(0, 10, 1, 0, \frac{1}{2}, -\frac{1}{2}, 0)$	$T_5(0, 10, 1, -\frac{1}{2}, 0, \frac{1}{2}, 0)$	

Table 11: *The chiral superfields are listed with their quantum numbers [38]. The F_i , \bar{f}_i , ℓ_i^c , as well as the h_i , h_{ij} fields and the singlets are listed with their $SU(5) \times U(1)' \times U(1)^4$ quantum numbers. Conjugate fields have opposite $U(1)' \times U(1)^4$ quantum numbers. The fields Δ_i and T_i are tabulated in terms of their $U(1)' \times SO(10) \times SO(6) \times U(1)^4$ quantum numbers.*

As can be seen, the matter and Higgs fields in this string model carry additional charges under additional U(1) symmetries [38]. There exist various singlet fields, and hidden-sector matter fields which transform non-trivially under the $SU(4) \times SO(10)$ gauge symmetry, some as sextets under SU(4), namely $\Delta_{1,2,3,4,5}$, and some as decuplets under SO(10), namely $T_{1,2,3,4,5}$. There are also quadruplets of the hidden SU(4) symmetry which possess fractional charges. However, these are confined and do not concern us further.

The usual flavour assignments of the light Standard Model particles in this model are as follows:

$$\begin{aligned} \bar{f}_1 &: \bar{u}, \tau, & \bar{f}_2 &: \bar{c}, e/\mu, & \bar{f}_5 &: \bar{t}, \mu/e, \\ F_2 &: Q_2, \bar{s}, & F_3 &: Q_1, \bar{d}, & F_4 &: Q_3, \bar{b}, \\ & & \ell_1^c &: \bar{\tau}, & \ell_2^c &: \bar{e}, & \ell_5^c &: \bar{\mu}, \end{aligned} \quad (55)$$

up to mixing effects which are discussed in more detail in [36]. We chose non-zero vacuum expectation values for the following singlet and hidden-sector fields:

$$\Phi_{31}, \bar{\Phi}_{31}, \Phi_{23}, \bar{\Phi}_{23}, \phi_2, \bar{\phi}_{3,4}, \phi^-, \bar{\phi}^+, \phi_{45}, \bar{\phi}_{45}, \Delta_{2,3,5}, T_{2,4,5}. \quad (56)$$

The vacuum expectation values of the hidden-sector fields must satisfy the additional constraints

$$T_{3,4,5}^2 = T_i \cdot T_4 = 0, \Delta_{3,5}^2 = 0, T_2^2 + \Delta_2^2 = 0. \quad (57)$$

For further discussion, see [36] and references therein.

Acknowledgements. M.E.G and S.L. are grateful to CERN for hospitality and support. S.L. would also like to thank the University of Huelva for kind hospitality. The research of S. Lola is co-funded by the FP6 Marie Curie Excellence Grant MEXT-CT-2004-014297. Additional support for research visits has been provided by the European Research and Training Network MRTPN-CT-2006 035863-1 (UniverseNet) and by the Greek Ministry of Education EPAN program, B.545. M.E.G. acknowledges support from the ‘Consejería de Educación de la Junta de Andalucía’, the Spanish DGICYT under contracts BFM2003-01266, FPA2006-13825 and the European Network for Theoretical Astroparticle Physics (ENTApP), member of ILIAS, EC contract number RII-CT-2004-506222.

References

- [1] Y. Fukuda et al., Super-Kamiokande Collaboration, Phys. Rev. Lett. 81 (1998) 1562, Phys. Rev. Lett. 82 (1999) 1810 and Phys. Rev. Lett. 82 (1999) 2430.
- [2] Q. R. Ahmad et al., SNO Collaboration, Phys. Rev. Lett. 87 (2001) 071301 and Phys. Rev. Lett. 89 (2002) 011301.
- [3] K. Eguchi et al., KamLAND Collaboration, Phys. Rev. Lett. 90 (2003) 021802; T. Araki et al., KamLAND Collaboration, Phys. Rev. Lett. 94 (2004) 081801.
- [4] M.H. Ahn et al., K2K Collaboration, Phys. Rev. Lett. 90 (2003) 041801.
- [5] D.G. Michael et al., MINOS colaboration, Phys. Rev. Lett. 97 (2006) 191801.
- [6] For an extensive list of references on the neutrino oscillation, reactor and accelerator data, and for related global fits, see: M. Maltoni, T. Schwetz, M.A.Tortola, J.W.F. Valle, New J. Phys. 6 (2004) 122; M.C. Gonzalez-Garcia, Phys. Scripta T121 (2005) 72.
- [7] See, for example, L. Wolfenstein, Phys. Rev. D17 (1978) 20; S.P. Mikheyev and A.Yu. Smirnov, Yad. Fiz. 42 (1985) 1441 and Sov. J. Nucl. Phys. 42 (1986) 913.
- [8] M. Apollonio et al., CHOOZ Collaboration, Phys. Lett. B338 (1998) 383; Phys. Lett. B420 (1998) 397.
- [9] For a review see W. Buchmuller, lectures at ESHEP 2001, Beatenberg, Switzerland, *Preprint hep-ph/0204288*.
- [10] F. Borzumati and A. Masiero, Phys. Rev. Lett. 57 (1986) 961.

- [11] For reviews, see: Y. Kuno and Y. Okada, Rev. Mod. Phys. 73 (2001) 151, J. Aysto et al., hep-ph/0109217, *Report of the Stopped Muons Working Group for the ECFa-CERN study on Neutrino Factory and Muon Storage Rings at CERN*.
- [12] G.C. Branco, R. Gonzalez Felipe, F.R. Joaquim and M.N. Rebelo, Nucl.Phys. B640 (2002) 202; G.C. Branco, R. Gonzalez Felipe, F.R. Joaquim, I. Masina, M.N. Rebelo and C.A. Savoy, Phys. Rev. D67 (2003) 073025; J. Ellis, J. Hisano, S. Lola and M. Raidal, Nucl.Phys. B621 (2002) 208; J. Ellis and M. Raidal, Nucl.Phys. B643 (2002) 229; T. Endoh, S. Kaneko, S.K. Kang, T. Morozumi, M. Tanimoto, Phys.Rev.Lett.89 (2002) 231601; S. Pascoli, S.T. Petcov and W. Rodejohann, Phys.Rev.D68 (2003) 093007; L. Velasco-Sevilla, JHEP 0310 (2003) 035.
- [13] C. D. Froggatt and H. B. Nielsen, Nucl. Phys. B147 (1979) 277.
- [14] L. Ibanez and G.G. Ross, Phys. Lett. B332 (1994) 100.
- [15] A very large number of neutrino mass and mixing patterns has been proposed in the literature. For a review, see G. Altarelli and F. Feruglio, Phys. Rept. 320 (1999) 295, and references therein.
- [16] See for instance S. Lola and G.G. Ross, Nucl. Phys. B553 (1999) 81, and references therein.
- [17] See for instance Y. L. Wu, Phys. Rev. D59 (1999) 113008; C. Wetterich, Phys. Lett. B451 (1999) 397; I. de Medeiros Varzielas, S.F. King and G.G. Ross, Phys. Lett. B644 (2007) 153 and hep-ph/0607045.
- [18] . S.F. King and G.G. Ross, Phys. Lett. B520 (2001) 243 and Phys. Lett. B574 (2003) 239.
- [19] For a review see R. N. Mohapatra *et al.*, hep-ph/0510213.
- [20] S. Antusch, J. Kersten, M. Lindner, M. Ratz and M.A. Schmidt, JHEP 0503 (2005) 024.
- [21] L. Covi, E. Roulet and F. Vissani, Phys. Lett. B384 (1996) 169; M. Plumacher, Nucl. Phys. B530 (1998) 207; M. Flanz and E.A. Paschos, Phys. Rev. D58, 113009 (1998); A. Pilaftsis, Int. J. Mod. Phys. A14 (1999) 1811; J. Ellis, S. Lola and D.V. Nanopoulos, Phys. Lett. B452 (1999) 87; W. Buchmuller and M. Plumacher, Int. J. Mod. Phys. A15 (2000) 5047; C.H. Albright and S.M. Barr, Phys. Rev. D70 (2004) 033013; G.C. Branco, M.N.Rebelo and J.I. Silva-Marcos, Phys. Lett. B633 (2006) 345.
- [22] B. Campbell, J. Ellis, J.Hagelin, D.V. Nanopoulos and K.A. Olive, Phys. Lett. B197 (1987) 355.
- [23] J. Ellis, D.V. Nanopoulos and K. Olive, Phys. Lett. B300 (1993) 121.
- [24] J.R. Ellis, S. Lola and D.V. Nanopoulos, Phys. Lett. B452 (1999) 87.
- [25] D.N. Spergel *et al.*, WMAP Collaboration, Astrophys. J. Suppl. 148 (2003) 175.
- [26] R. Barbieri, P. Creminelli, A. Strumia and N. Tetradis, Nucl. Phys. B **575** (2000) 61; T. Endoh, T. Morozumi and Z. h. Xiong, Prog. Theor. Phys. **111** (2004) 123; A. Pilaftsis and T. E. J. Underwood, Phys. Rev. D **72** (2005) 113001.

- [27] A. Abada *et al.*, JCAP 0604 (2006) 004 and JHEP 0609 (2006) 010; O. Vives, Phys. Rev. D 73 (2006) 073006; A. de Simone and A. Riotto, JCAP 0702 (2007) 005; S. Blanchet and P. Di Bari, JCAP 0703 (2007) 018.
- [28] J. Hisano, T. Moroi, K. Tobe, M. Yamaguchi and T. Yanagida, Phys. Lett. B357 (1995) 579; J. Hisano, T. Moroi, K. Tobe and M. Yamaguchi, Phys. Rev. D53 (1996) 2442; M.E. Gomez and H. Goldberg, Phys. Rev. D53 (1996) 5244; J. Hisano and D. Nomura, Phys. Rev. D59 (1999) 116005.
- [29] S. Lavignac, I. Masina and C.A. Savoy, Phys. Lett. B520 (2001) 269 and Nucl. Phys. B633 (2002) 139.
- [30] J. R. Ellis, J. Hisano, M. Raidal and Y. Shimizu, Phys. Lett. B528 (2002) 86.
- [31] P.H. Chankowski, J.R. Ellis, S. Pokorski, M. Raidal and Krzysztof Turzyski, Nucl.Phys. B690 (2004) 279.
- [32] G.L. Kane, S.F. King, I.N.R. Peddie and L. Velasco-Sevilla, JHEP 0508 (2005) 083.
- [33] G. Altarelli and F. Feruglio, Phys. Lett. B451 (1999) 388.
- [34] S. F. King, JHEP 0209 (2002) 011.
- [35] T. Banks, Nucl. Phys. B303 (1988) 172; L.J. Hall, R. Rattazzi and U. Sarid, Phys. Rev. D50 (1994) 7048; M. Carena, M. Olechowski, S. Pokorski, and C.E.M. Wagner, Nucl. Phys. B426 (1994) 269; E.G. Floratos, G.K. Leontaris and S. Lola, Phys. Lett. B365 (1996) 149; M.E. Gomez, T. Ibrahim, P. Nath and S. Skadhauge, Phys. Rev. D70 (2004) 035014.
- [36] J. Ellis, G.K. Leontaris, S. Lola and D.V. Nanopoulos, Phys. Lett. B425 (1998) 86.
- [37] J. Ellis, G.K. Leontaris, S. Lola and D.V. Nanopoulos, Eur. Phys. J. C9 (1999) 389.
- [38] I. Antoniadis, J. Ellis, J. Hagelin and D.V. Nanopoulos, Phys. Lett. B194 (1987) 231 and Phys. Lett. B231 (1989) 65.